HEINCKE-Berichte

Gas system within Svalbard's fjords

Cruise no. HE628

04 September – 01 October 2023
Longyearbyen (Norway) – Stavanger (Norway)
FJORDGAS

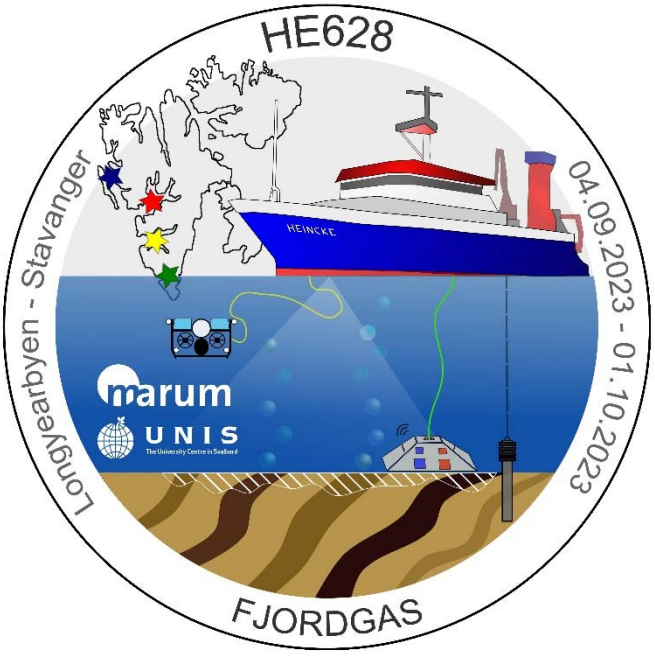

AUTHORS

Römer M, Marcon Y, Pape T, Malnati J, Meurer C, Gutiérrez Flores P, Bazhenova E, Feddersen G, Marklein M, Betlem P, Rodes N

Miriam Römer
University of Bremen, MARUM

2024

Table of Contents

1 Cruise Summary

1.1 Summary in English

This cruise report details the findings and outcomes of the FJORDGAS expedition, a comprehensive investigation of the gas system in the western fjords of Svalbard conducted aboard the research vessel R/V HEINCKE. The expedition commenced on September 4th 2023, with a focus on mapping seafloor gas bubble discharge within Spitsbergen's western fjords. The study aimed to quantify gas emissions, understand spatial distributions, and investigate the correlation between emission sites and geological units. The research employed hull-mounted echosounders for mapping, CTD rosettes, gravity corers, and a multicorer for sample collection, a MiniROV and a sonar lander. Methane concentrations in water and sediment samples were analyzed onboard and indicate the occurrence of localized, near-surface methane enrichments. The miniaturized ROV provided images of seepage areas, revealing microbial mats and carbonate precipitates. The HE628 cruise employed a systematic hydroacoustic mapping approach, covering predefined boxes targeting geological units. Results indicated concentrated gas emissions in specific areas correlated with geological formations. The expedition also explored an oil seep area offshore Prins Karls Forlandet, confirming a natural release of oil-coated bubbles. Additional exploration in Van Mijenfjorden and Van Keulenfjorden unveiled varying gas emission intensities, with suspected temporal influences from local tides. Furthermore, measurements of methane concentrations in discrete water samples taken at flare sites and in the air (continuous measurements) have been conducted to evaluate the fate of the hydrocarbons released.

The FJORDGAS expedition contributes valuable insights into the complex dynamics of gas seep systems in the Svalbard fjords, emphasizing the importance of geological factors and providing a foundation for future studies on gas emissions in Arctic marine environments.

1.2 Zusammenfassung

Dieser Fahrtbericht beschreibt die Ergebnisse der FJORDGAS-Expedition, einer umfassenden Untersuchung des Gassystems in den westlichen Fjorden Spitzbergens, die an Bord des Forschungsschiffs HEINCKE durchgeführt wurde. Die Expedition begann am 4. September 2023 und konzentrierte sich auf die Kartierung der Gasblasenaustritte am Meeresboden in den westlichen Fjordsystemen von Spitzbergen. Ziel der Studie war es, die Gasemissionen zu quantifizieren, die räumliche Verteilung zu verstehen und die Korrelation zwischen Methanemissionen und geologischen Einheiten zu untersuchen.

Für die Forschung wurden an Bord montierte Echolote zur Kartierung, CTD-Rosetten, Schwerelot und ein Multicorer zur Probenentnahme, ein MiniROV und ein Sonar-Lander eingesetzt. Die Methankonzentrationen in Wasser- und Sedimentproben deuten auf lokale, oberflächennahe Anreicherung von Methan hin. Das miniaturisierte ROV lieferte Bilder vom Meereboden, die mikrobielle Matten und Karbonatausfällungen an den Emissionsstellen erkennen ließen. Auf der HE628 wurde ein systematisches hydroakustisches Kartierungsverfahren mit vordefinierte Boxen angewandt, welche die geologischen Einheiten abdeckten. Die Ergebnisse zeigten konzentrierte Gasemissionen in bestimmten Bereichen, die mit geologischen Formationen korrelierten. Die Expedition untersuchte auch ein Ölaustrittsgebiet vor der Küste von Prins Karls Forlandet und bestätigte eine natürliche Freisetzung von ölumhüllten Blasen. Weitere Untersuchungen im Van Mijenfjorden und Van Keulenfjorden ergaben unterschiedliche Intensitäten der Gasemissionen, die vermutlich durch die Gezeiten beeinflusst werden. Darüber hinaus wurden Messungen der Methankonzentration in diskreten Wasserproben an den Austrittsstellen und in der Luft (kontinuierliche Messungen) durchgeführt, um den Verbleib der freigesetzten Kohlenwasserstoffe zu untersuchen.

Die FJORDGAS-Expedition liefert wertvolle Einblicke in die komplexe Dynamik der Gasaustrittssysteme in den Fjorden Spitzbergens, unterstreicht die Bedeutung geologischer Faktoren und bietet eine Grundlage für künftige Studien über Gasemissionen in der arktischen Meeresumwelt.

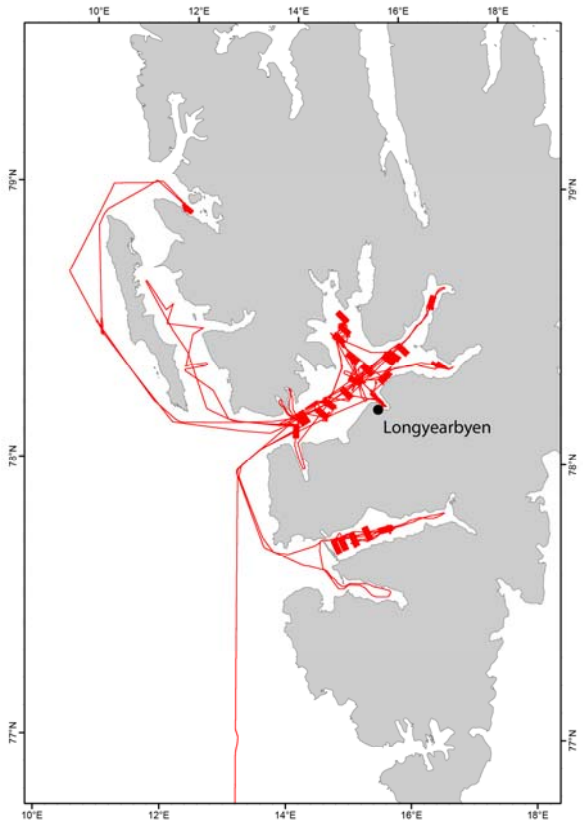

Fig. 1.1: Cruise track of HE626 (red line) in the work area in Svalbard.

2 Participants

2.1 Principle Investigators

Name	Institution
Marcon, Yann, Dr.	GeoB/MARUM
Noormets, Riko, Prof.	UNIS
Pape, Thomas, Dr.	GeoB/MARUM
Römer, Miriam, Dr.	GeoB/MARUM

2.2 Scientific Party

Name	Discipline	Institution
Bazhenova, Evgenia	Hydroacoustics	MARUM
Betlem, Peter	Hydroacoustics	UNIS
Feddersen, Greta	Gas geochemistry	GeoB
Gutierrez Flores, Pablo	Mini ROV	MARUM
Malnati, Janice	Gas geochemistry	GeoB
Marcon, Yann	Sonar Lander	GeoB/MARUM
Marklein, Max	Gas geochemistry	GeoB
Meurer, Christian	Mini ROV	MARUM
Pape, Thomas	Gas geochemistry	GeoB/MARUM
Rodes, Nil	Hydroacoustics	UNIS
Römer, Miriam	Chief scientist	GeoB/MARUM

Fig. 2.1: Scientific crew participating HE628 on R/V HEINCKE.

2.3 Participating Institutions

GeoB Fachbereich Geowissenschaften der Universität Bremen, Klagenfurter Straße, D-28359 Bremen, German, https://www.geo.uni-bremen.de

MARUM Zentrum für Marine Umweltwissenschaften, Universität Bremen, Leobener Straße, D-28359 Bremen, Germany, http://www.marum.de

UNIS The University Center in Svalbard, Longyearbyen, Norway, https://www.unis.no

3 Research Program

3.1 Aims of the Cruise

The overarching aim of the cruise was to quantitatively and qualitatively investigate the gas system within Svalbard's fjords. Based on our previous studies, we suggest to characterize the nature of the active gas system within Svalbard's western fjords, including the quantity of emitted methane, the gas source and fate and further ground truth the presence of gas hydrates in shallow sediments in the deepest parts of the fjords. A better knowledge about near-seabed fluid flow and seepage within fjord systems would be needed to evaluate the importance for gas exchange and fluid fluxes from the seafloor into the water column and eventually into the atmosphere.

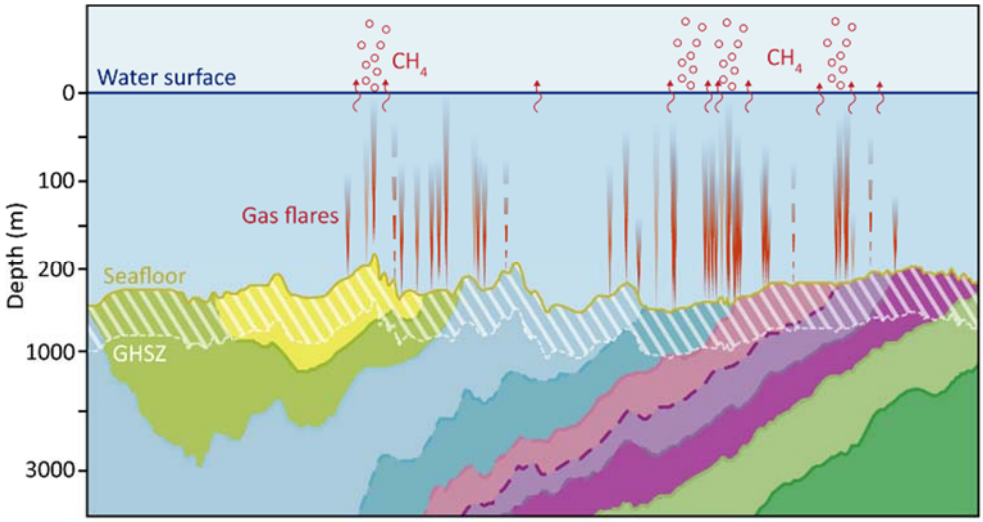

Fig. 3.1: Graphical illustration of the five main objectives for better understanding of the gas and seepage system in Svalbard's fjords. Numbers refer to specific aims described here.

AIM 1: Gas emission distribution and geological control

- Systematic mapping allows to constrain the distribution of gas bubble sources at the seafloor and possibly reveal a relation to the subsurface geological units and structures.
- Near-coast detected seepage might be related to trapping permafrost present in the subsurface. Verifying and monitoring such a relation would be crucial to assess whether future permafrost decrease due to ocean warming will lead to stronger gas emissions.

AIM 2: Temporal and spatial variability of gas ebullition

- First results from past expeditions showed that flares were not stable over hours and days. Better understanding about the variability and the controlling factors is crucial to evaluate the gas quantities released.

AIM 3: Hydrocarbon source(s)

- What is the origin of the light hydrocarbons (predominantly methane) in the gas emissions detected? Gas samples taken directly at the seeps sites at the seafloor allow constraining the hydrocarbon source(s) from gas composition and isotopic investigations. The gas composition is crucial for modelling the gas hydrate stability zone.

AIM 4: Gas hydrate sampling or indirect verification of their presence in fjord sediments

- Modelling of the GHSZ predict the formation of gas hydrates in shallow sediments provided gas and water availability (Fig. 3.2) at stable pressure and temperature conditions. Flare findings in the water column indicate that gas is indeed available in the sediments,

but physical evidence of gas hydrate saturated sediments is still lacking. We intend to sample intact gas hydrates in shallow sediments by gravity coring. In the event that hydrates will have been dissociated during core recovery, their in-situ existence will be proven by indirect indications like anomalies of sediments temperatures (infrared camera) or chloride concentration anomalies in extracted pore waters.

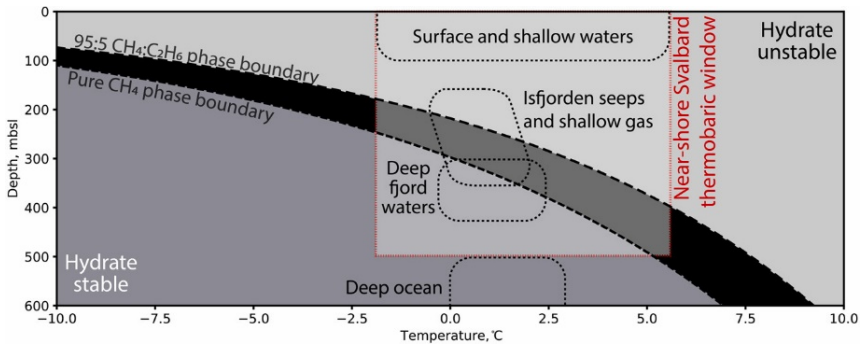

Fig. 3.2: Schematic illustration of the estimated GHSZ (for pure CH_4 and a mixture of CH_4:C_2H_6 of 95:5) in Svalbard's fjords. Figure from Betlem et al. (2021).

AIM 5: Quantities of methane released through gas bubbles and possible contribution to atmospheric methane inventory

- How much bubble-forming gas is released from the seafloor? In order to answer this question, a combination of visual analysis including size measurements and release frequencies (e.g. Römer et al., 2012) and models based on split-beam echosounders for calculating the backscatter response of single bubbles to calculate the gas flow rate (Veloso et al., 2015) would lead to a first estimate of quantities.
- Does methane released from the seafloor reach the sea-air interface and contribute to the atmospheric inventory, at various water depths, and varying conditions, such as, near-coastal, inner-fjord settings, mouth of fjords? Measurements of methane concentrations in discrete water samples taken at flare sites and in the air (continuous measurements) are needed to evaluate the fate of the hydrocarbons released.

3.2 Agenda of the Cruise

Following our objectives listed above, we proposed a work program, which consists of a) an initial systematic flare mapping (AIM 1), b) studies of the variability of detected gas emissions (AIM 2), c) sampling of gas bubbles and visual investigations of the seafloor (AIM 3), d) sampling of shallow sediment and gas hydrate (AIM 4), and e) investigations of the fate of released light hydrocarbons (AIM 5).

a) Systematic flare detection and localization with hydroacoustic methods

Surveys with the ship-based Kongsberg EM710 swath echosounder and the Simrad EK80 split-beam echosounder will be conducted to systematically map hydroacoustic anomalies in the water column (flares) indicative for seafloor gas emissions. Release of gas bubbles injected to the water column can be detected with different hydroacoustic systems due to an impedance contrast between free gas and the surrounding water column. Most commonly single beam echosounders such as the parametric parasound echosounder (Römer et al., 2012) or the split-beam echosounder Simrad EK60 (Westbrook et al., 2009) were successfully used for the detection of bubble streams.

Recent advancements in the water column imaging, data recording, and processing capabilities of multibeam echosounders like Kongsberg EM710 (e.g. Schneider von Deimling et al., 2007) make these systems the first choice for gas emission imaging. Multibeam echosounders have the advantage of imaging gas emissions over a much wider swath compared to single beam systems, and, ping-by-ping, in three dimensions. This provides more detailed information on the origin of gas emissions at the seafloor, their deflection during ascent and overall rising heights. Due to geometric reasons and strong noise in the outer beams, the area for flare detection is however significantly smaller than for bathymetric mapping. Besides a narrow line spacing, the vessel speed needs to be reduced to ~5 kn for an enhanced resolution to be able to clearly identify flares. The multibeam system as well as the towed EdgeTech sidescan will additionally be used to detect seafloor backscatter anomalies, caused due to near-surface occurrence of gas hydrates, authigenic carbonates or high gas concentrations in the sediments. Finally, subbottom records (i.e. SES2000 and towed EdgeTech) will enable detection of areas of high gas content in the sediments that are characterized by blanking zones.

b) Spatial and temporal variability studies

In order to investigate flare variability over different years, we plan to repeat parts of the surveys conducted during cruises HE449, HE450 in 2015, and the R/V Clione cruise in 2021. The latter was limited to shallow waters in Isfjorden, however, revealed differences with the 2015 data set. In addition, individual flares will be monitored repeatedly with ship echosounders. For more continuous monitoring, a Sonar Lander will be deployed next to a seep site, where it should scan the emissions every five minutes for several days (depending on weather conditions for recovery). Long-term monitoring is necessary to study the mechanisms that control seabed gas release (Marcon et al., 2019). The results will help to investigate trigger mechanisms for activity and seep intensity. It has been shown that tides have an important influence on seep activity (e.g. Römer et al., 2016; Marcon et al., 2021), however, recent deployments of the Sonar Lander indicate that other factors additionally affect the seep intensity. A better understanding of seep variability is urgently needed to improve quantitative measurements of fluid flow from the seafloor into the water column.

c) Gas sampling and visual seep investigations with MiniROV

Gas bubbles will be sampled from different seep sites using a small size MiniROV. Two samples can be taken during each dive revealing gas in sufficient amounts for the analysis of hydrocarbon concentrations and C and H isotopes of methane of each sample. We intend to take the samples from seep sites located at different outcropping geological formations to identify formation-related variations in gas compositions. So far, the MiniROV is rated to 100 m water depth (which affects sampling mainly in deeper parts of Isfjorden and its tributary fjords), but, it is planned to improve the maximum deployment depths. For deeper areas inaccessible with the MiniROV, sediment sampling and subsequent analysis of methane and other diagnostic ingredients in extracted pore waters will be conducted. During MiniROV dives for sampling, seep areas will be visually inspected and reveal if seep indicators like microbial mats, other seep biota, or darkish colored reduced sediments accompany the emission sites. Furthermore, seafloor areas characterized by pockmarks will be investigated, as those were suggested to have formed as a result of sedimentary fluid flow (Roy et al., 2015).

d) Gas hydrate sampling and quantification

Following the systematic flare detection by hydroacoustics gravity cores equipped with transparent plastic foil liners will be collected at the potential gas hydrate locations to visually prove the presence of hydrates. The core recovery and sampling procedure needs to be fast as the gas hydrates start to decompose when the sediment core is moved out of the gas hydrate stability field. An infrared camera will be used to illustrate if temperature anomalies indicate the presence of dissociating gas hydrate. After opening the core, intact gas hydrate pieces will be transferred into plastic syringes for controlled dissociation. The released gas will be transferred into glass vials filled with NaCl solution for on board analysis of molecular compositions by gas chromatography. Sediment samples from gravity cores will be transferred immediately after recovery into glass vials filled with NaOH solution for the onboard analysis of concentrations of dissolved methane applying the headspace technique (gas chromatography). Pore water samples will be extracted from the sediments with rhizons and analyzed for concentrations of dissolved sulfide, sulfate, and chloride to verify the presence of gas hydrates. As chloride is an abundant and conservative ion in pore waters of shallow marine sediments, changes in dissolved chloride content can be used to monitor formation and decomposition of gas hydrate deposits (Bohrmann & Torres, 2006).

e) Fate of the released light hydrocarbons

As an essential extension to our previous work, continuous air measurements with the ICOS system installed on-board will show immediately, if methane is transported through gas bubbles into the atmosphere. Flares detected during earlier cruises partly reached surface waters. However, the fraction of methane remaining in the bubbles in near-surface waters is not yet known. In addition, discrete water sampling at selected flare sites will show the distribution of dissolved methane concentrations through the entire water column. The hydrocasts will further reveal, if water column stratification is influencing the fate of dissolved methane and inhibiting gas transfer at the sea-air interface.

Measures to conduct responsible marine research

The planned research activities have been carried out in accordance with the declaration on responsible marine research. During the introduction meeting the scientists on board were sensitize to the topic. Regarding “Mitigation measures for the operation of seismic and hydroacoustic sources with pulsed sound emissions” we declared that the use of multibeam echosounder, subbottom profiler as well as sidescan sonar has been limited to the level strictly necessary for scientific purposes. Before a source was first triggered, in daylight and adequate visibility, operators scanned the area around the vessel up to a distance of 500 m (mitigation radius) for marine mammals from a suitable position for a period of 60 minutes. Measurements only commenced if no marine mammals were observed within the mitigation radius.

3.3 Description of the Work Area

The working area is located offshore Svalbard. For the proposed cruise, we defined six study areas (Fig. 3.3): Area 1) Isfjorden, Area 2) Kongsfjorden/Krossfjorden, Area 3) Van Mijenfjorden/Van Keulenfjorden, Area 4) Hornsund, Area, 5) Prins Karls Forland, 6) Forlandssundet.

Our main work area is Isfjorden and its tributary fjords including Adventfjorden, Grønfjorden, Nordfjorden, Billefjorden, Sassenfjorden and Tempelfjorden (Fig. 3.4). Flares have been detected widely distributed in this area (Fig. 3.4)

Van Mijenfjorden is the second largest fjord along western Spitsbergen, and the presence of flares has been confirmed during cruise HE449 in 2015 (Fig. 3.3). Van Keulenfjorden in contrast was not investigated in this regard prior to HE628. However, flares would be expected to be related to Jurassic – Cretaceous outcrops, similarly to the first findings within Van Mijenfjorden (Fig. 3.3), which would strengthen the interpretation of a geologic control of flare distribution.

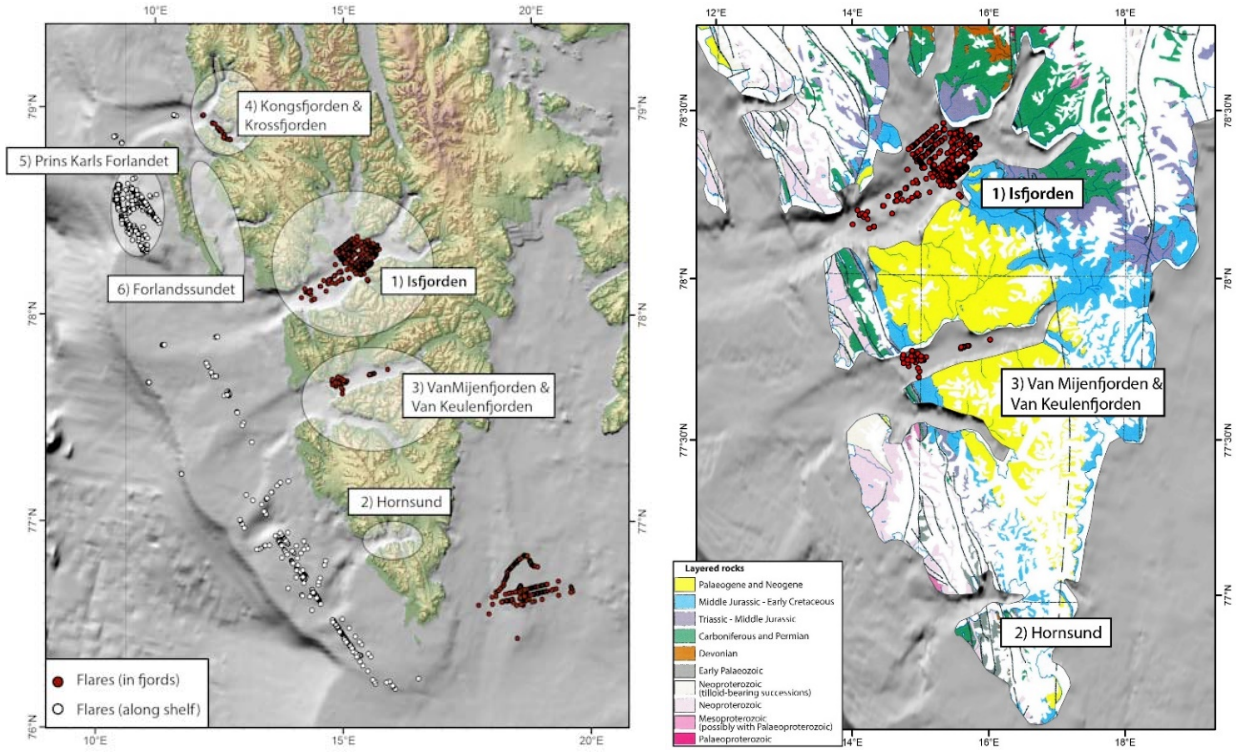

Fig. 3.3: Left: Map including the six planned work areas. Right: Stratigraphic map of Svalbard focusing on planned work areas 1, 2 and 3.

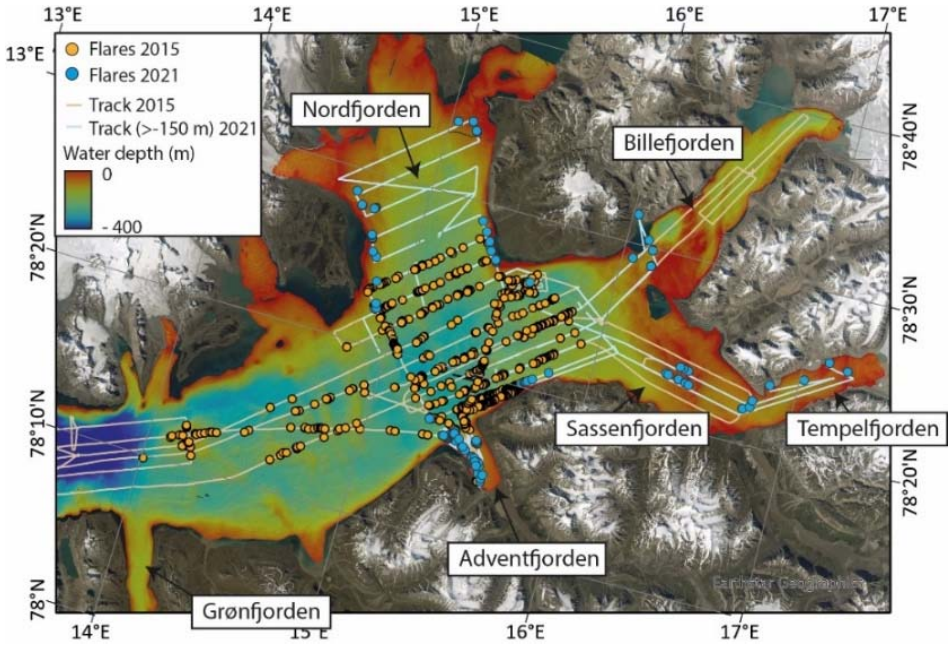

Fig. 3.4: Overview of Isfjorden and its tributary fjords proposed to be investigated in detail.

4 Narrative of the Cruise

We started our expedition to investigate the gas system in the western fjords of Svalbard (FJORDGAS) on research vessel R/V HEINCKE in Longyearbyen, Spitsbergen, in the morning of Monday, September 4th. All scientists and some crew members arrived two days earlier in order to receive the equipment including sampling gears and laboratory equipment, to install it on board and securely lash it. We were warmly welcomed by the crew and started highly motivated to our sampling and mapping campaign. We started our investigations within Spitsbergen's Isfjorden immediately after having left the port of Longyearbyen, and systematically mapped the water column for seafloor gas bubble discharge with the ships echosounders. Numerous gas emissions were detected already since the beginning of our mapping. In order to quantify the amount of released gas we systematically map selected areas in different parts of the fjords and attempt to understand the controlling factors for the spatial distributions of gas emissions. We hypothesized that gas emission sites are correlated with outcropping geological units. Indeed, our dense mapping strategy applied shows that the gas emissions are not randomly distributed in all parts of Isfjorden, but are concentrated in specific areas. In addition to mapping with the hull-mounted echosounders, several individual gas emission sites were investigated. Water samples and sediment samples were collected with a CTD rosette, a gravity corer and a multicorer, respectively. The multicorer we use was loaned by the Alfred-Wegener-Institute, Bremerhaven, and provided us some high-quality sediment cores of undisturbed near-seafloor sediments of about half a meter in length. The gravity corer allows to sample deeper sediments with cores up to 6 m in length. Methane concentrations of water and pore water samples were already determined onboard, whereas other properties of the sediment cores, such as lithologies and concentrations of pore water ingredients will be analyzed after the cruise in the home laboratories. The results obtained on board allow us to directly evaluate the suitability of the sampled location to discuss further strategies. Because the extent of individual seafloor gas emission sites is restricted, precise seafloor sampling is needed. R/V HEINCKE lacks a dynamic positioning system, but the captain and the nautical officers have done a great job and proven their skills in positioning the sampling devices in meter precision to our sampling targets. Nevertheless, sampling seep areas is still challenging. In areas fueling flares, we encountered dense accumulations of precipitates, which drastically hampered penetration of the gravity corer.

During the second week of research cruise HE628 we acquired large amounts of new hydroacoustic data and collected sediment and water samples from multiple methane seepage areas successfully that increased our understanding of the gas seep system in Isfjorden. Following a systematic approach we investigated various geological units outcropping at the seafloor that were previously mapped using seismic surveys by our collaborators at UNIS, the University Center in Svalbard. It has been shown prior to our cruise that the distribution of gas emissions is likely controlled by the underlying strata. The goal of our investigations is to methodically map the gas seep distribution in relation to the geological background in order to quantitatively investigate the intensity of the gas release within the western fjords. The most intense gas emissions detected in each geological unit were then sampled to analyse the gas source. A miniaturised remotely operated vehicle (ROV), built and adapted by MARUM to investigate and sample gas seeps in water depths down to 300 m, provided the first images of some of the seepage areas. Our first dives to seeps in Isfjorden showed microbial mats at the seafloor and also that carbonate precipitates occur even exposed at the seafloor where gas bubbles are released into the water column. The occurrence of carbonate precipitates makes sediment sampling difficult, as neither

the gravity corer nor the multicorer could penetrate through these hard carbonate layers. Nevertheless, using the underwater acoustic positioning system (GAPS) of R/V HEINCKE we were able to target sampling locations at the seafloor with meter precision and to collect cores right next to the carbonate while still within the seepage areas. These cores contained high amounts of methane, both in dissolved and gaseous phases, and underwent intense degassing when brought on deck.

On Tuesday, September 12th, we left Isfjorden to investigate a recently detected oil seep area on the shelf offshore Prins Karls Forlandet. The oil release was first discovered from satellite images, which showed a recurring oil slick at the sea surface. ROV investigations from colleagues from the UiT Arctic University of Norway in Tromsø confirmed that the surface slick originated from a natural release of oil-coated bubbles at the seafloor. We mapped the area systematically using our hydroacoustic systems and investigated the differences between the oil-coated bubble emissions and other nearby gas bubble emissions without oil leakages. During mapping and sampling stations in that area, we could observe the oil slick and even spot oil-coated bubbles popping up at the sea surface and forming circular oily patches. Our collaborator from the Norwegian Petroleum Directorate (NPD) provided us with the most recent satellite images, including one taken on the day of our investigations, which showed not only the oil slick that we had observed but also our vessel R/V HEINCKE next to it.

After investigating the oil release at the shelf, another target was to look for active gas seepage inside Kongsfjorden, specifically in the vicinity of Ny Ålesund. The presence of gas seepage in this area had been suggested from previous surveys conducted in 2015 with R/V HEINCKE. Surprisingly, despite intense surveying during September 13th, we couldn't detect any sign of gas release in that area. We decided therefore to transit back to Isfjorden and resume our methodical mapping and sampling approach. After deploying our sonar lander on Saturday morning, September 16th at one of the most intense flare clusters we detected so far in Isfjorden, we headed towards Van Mijenfjorden. The sonar lander recorded continuous data for five days that will be used for variability studies of the gas emissions. Between Spetember 16th and September 19th, we investigated the seep system in Van Mijenfjorden to compare these observations with our results from Isfjorden. Partly the same geological formations are present in this fjord, and first investigations today have proven already that an active gas seep system does exist in Van Mijenfjorden.

On Tuesday, September 19th we completed all planned mapping surveys and sampling stations in Van Mijenfjorden. Preliminary observations show that the gas emission activity appears to be less intense in this fjord compared to Isfjorden but temporally variable. We suspect that gas release here may be influenced by the local tides, as also known from other seep areas. Our investigations in Van Mijenfjorden were followed by a brief explorative mapping in the neighbouring Van Keulenfjorden on September 19th. In this fjord we detected for the first time the presence of gas bubble emissions from the seafloor into the water column. In the afternoon of the 19th, we celebrated the "Bergfest", which traditionally marks the halfway point of the cruise. Both the ship crew and the scientific party could then had a barbecue on the working deck near the entrance of the fjord. Although the temperatures were around zero degree Celsius, we enjoyed the view towards Svalbard's snow covered mountains during the long lasting sunset. It was also a good opportunity to thank the crew for their full support, since our expedition would not be possible without their help. Such a great assistance as we experienced here during this cruise is exceptional and it is a pleasure for us to work on R/V HEINCKE!

After our return to Isfjorden, we recovered the sonar lander on September 20th that was deployed five days earlier at the seafloor. The sonar lander is an autonomous, battery-powered instrument designed to monitor the variations of methane gas emissions from the seabed over several days. During operations, the sonar lander was set to conduct one scan every five minutes, which will allow for analysis of a tidal influence of the gas bubble emission. Aside from the sonar, a camera and a CTD probe were mounted to the lander. It has been deployed four times during HE628 within three different seep areas in Isfjorden. First analysis of the data confirmed the varying intensities of the observed seep sites, whereas gas activity was continuous and never stopped entirely during the days of observation. Detailed analysis in combination with the CTD data will follow back home.

On September 24th, we finished our last station and hydroacoustic survey in the fjords of Svalbard. Part of the scientific crew disembarked in Longyearbyen, while the other part transited on R/V HEINCKE southwards to Stavanger, where the cruise ended. As soon as part of the scientific crew disembarked in Longyearbyen on Sunday 24th, we started the transit journey towards Stavanger. Because of forecasts announcing stormy conditions, we headed straight south after leaving Isfjorden, with the hope of covering as much distance as possible ahead of the storm. The beginning of the transit was dedicated to packing all scientific equipment that was not needed anymore. The Monday 25th was relatively calm and allowed everyone on board to ensure that all equipment and boxes were properly latched and secured. As announced, we encountered a severe storm during the night from Monday to Tuesday, with waves up to about 6-7 m high, which lasted until Thursday morning. After several weeks of perfectly calm sea conditions around Svalbard, many of us were unaccustomed to such conditions and had hard times adjusting to them. The initial plan was to take advantage of the transit journey to Stavanger to conduct a multibeam survey and search for seabed gas emissions in the shelf-slope area near the Lofoten-Vesterâlen Ocean Observatory off the Norwegian coastline. Unfortunately, this plan had to be abandoned due to the bad sea conditions in this area and also because the storm had slowed us down considerably. Instead, we kept steaming towards Stavanger. After slightly calmer conditions on Thursday and Friday, we encountered another storm in the night to Saturday and finally arrived in Stavanger safely and as scheduled on Sunday morning, October 1st. The last day on board was spent to finalizing the packing of all equipment as well as to cleaning the laboratories and the cabins before the HE629 scientist party came onboard on October 2nd.

5 Preliminary Results

5.1 Systematic Mapping Approach Related to Local Geology

Svalbard's fjord and onshore geology consist of thick sedimentary units comprising both hydrocarbon source and reservoir rocks. There have been documented instances of secondary and tertiary migrated hydrocarbons in both Svalbard's onshore (Abay et al., 2017; Ohm et al., 2019) and offshore settings (Roy et al., 2019; Rodes et al., 2023). Multiple technical gas discoveries (predominantly methane) have been made in Late Palaeozoic-Mesozoic successions (Senger et al., 2019, and references therein). The Middle Triasic Botneheia Formation and the Upper Jurassic to Lower Cretaceous Agardhfjellet Formation are regional organic rich source rocks (Abay et al., 2017; Ohm et al., 2019; Senger et al., 2019) and have time-equivalent stratigraphic intervals that represent major source rock for many oil and gas fields across the Norwegian continental shelf (Spencer et al., 2008).

Regional seismic profiles, a multitude of coal and petroleum boreholes, and excellent outcrop exposures provide good constraints on the archipelago's geology. Outcrop-Borehole-Seismic integration further facilitates onshore-offshore correlations, including the offshore mapping of geological unit boundaries and structural features. In addition, geomorphological features have been extensively mapped across Svalbard's fjords, i.e. thousands of pockmarks have previously been mapped (Roy et al, 2015). These were hypothesised to be related to palaeo and modern fluid seepage, though more recent work by Rodes et al. (2023) found no clear correlation between pockmark occurrence and the ongoing seepage patterns observed during the HE449 (2015) and GASGEM (2021) cruises.

HE628 employed a systematic mapping approach to better correlate the flares with the regional geology. Hydroacoustic mapping along pre-defined, equisized boxes (5 km x 12 lines grid with 200 m line separation) targeted the geological units defined by Rodes et al. (2023) to constrain the distribution of gas seepage sources across units and morphological expressions. Each geological unit contained at least one mapping box. Equivalent geological units were targeted in both Isfjorden and Van Mijenfjorden, covering exposures in both the western and eastern flank of the exposed Central Spitsbergen Basin. Explorative surveys further targeted otherwise unexplored fjord tributaries, typically along semi-parallel inward and outward profiles along different depth profiles. Along with opportunistic mapping during transits, this provided clues on the temporal aspects of gas seepage and the wider occurrence of offshore gas seepage. Temporal changes in flaring were also addressed through the partial remapping of Box 2, which was mapped both at the start and towards the end of the HE628 cruise.

In total, 25 mapping boxes for hydroacoustic mapping have been conducted during HE628 (Table 5.1.1). The mapping boxes were consecutively numbered but did not correspond to individual days or working areas.

Table 5.1.1 List of the mapping boxes surveyed during HE628.

Box	Fjord	Geological unit	Multibeam	EK80	Subbottom
1	Isfjorden	Kapp Toscana Group	X	X	X
2	Isfjorden	Agardhfjellet Formation	X	X	X
3	Isfjorden	Kapp Toscana Group	X		
4	Nordfjorden	Sassendalen Group	X	X	X
5	Nordfjorden	Sassendalen Group	X		X

6	Nordfjorden	Tempelfjorden Group	X		
7	Isfjorden	Janusfjellet Subgroup	X		X
8	Isfjorden	Adventdalen Group	X	X	X
9	Isfjorden	Tempelfjorden Group	X		
10	Isfjorden	Sassendalen Group	X		
11	Isfjorden	Van Mijenfjorden Group	X	X	X
(12)	Isfjorden	Van Mijenfjorden Group	(X)		
13	Isfjorden	Adventdalen Group	X	X	X
14	Isfjorden	Janusfjellet Subgroup	X		
(15)	Isfjorden	several	(X)		
16	Isfjorden	Sassendalen Group	X		
17	Van Mijenfjorden	Janusfjellet Subgroup	X	X	X
18	Van Mijenfjorden	Adventdalen Group	X	X	X
19	Van Mijenfjorden	Van Mijenfjorden Group	X	X	X
20	Van Mijenfjorden	Van Mijenfjorden Group	X		
21	Van Mijenfjorden	several	X		
22	Isfjorden	Van Mijenfjorden Group	X		
23	Isfjorden	Gipsdalen Group	X		X
24	Isfjorden	Kapp Toscana Group	X	X	X
25	Sassenfjorden	Gipsdalen Group	X		X

5.2 Mapping of the Seafloor by Multibeam

Data acquisition

Bathymetric mapping was performed using the Kongsberg EM712 multi-beam echosounder integrated with the motion and positioning systems onboard R/V HEINCKE. The system operated almost continuously throughout the cruise. Raw bathymetry (.kmall) and water column (.kmwcd) data were recorded using the Kongsberg SIS v.5.11.1 software package. The multibeam was set with equidistant beam separation and dynamic dual swath. Real-time data plotting allowed for the data coverage and quality control. As surveyed depths ranged from 20 to 430 m, SIS depth modes “Very Shallow” and “Shallow” were used. “Shallow” mode was used for the majority of the surveys, while Very Shallow mode was applied in depths shallower than 120 m for quality increase. During mapping boxes and exploratory transects, the vessel's operating speed was fixed at 5 kn, while it increased to a maximum speed of 7-8 kn during transits. Significant acoustical interference with the sub-bottom profiler (operating at 4 kHz) was observed at depths below 200 m. SBP profiling was normally disabled during mapping the planned boxes in order to reduce the noise level in the water column.

Sound velocity measurements

Hull-mounted sound velocity sensor Valeport miniSVS was used to provide real-time sound velocity measurements at the MBES transducer head. Vertical sound velocity profiles (SVP) were collected using the Valeport MIDAS SVP probe at 15 chosen locations withing mapping boxes (for location coordinates see Ch. 6 Station list), to correct the acoustic ray tracing for the water column stratification during the data acquisition. If the SVP collection was not possible prior to

start of a new mapping box, the appropriate SVP data were applied during the postprocessing. At station 38, no SVP data were collected because of the CTD data available. In this case, the speed of sound was recalculated as a function of temperature, salinity and depth utilizing the Mackenzie equation (1981).

Vertical datum

No tidal corrections were applied during the data acquisition or data postprocessing. However, water-level variations were observed during the mapping. For example, in Van Mijenfjorden a change of ca. 1 m was observed during two days while mapping different parts of Box 20.

Data postprocessing

Raw bathymetry data (.kmall) were imported into the QPS Qimera software v.2.5.3. Achieved sounding density at different depths allowed for gridding data at 2-4 m horizontal resolution. Initial quality control included 1) verification that the SVP data were applied correctly based on the time and location; 2) filtering of the outliers using the weak spline, 3) manual point cloud cleaning if required. Additional cleaning is required for bathymetry data collected simultaneously with sub-bottom profiling.

Preliminary results

Preliminary bathymetric grids were created for all the mapping boxes (Fig. 5.2.1) and exported as georeferenced .tiff files. Additionally, a combined grid was created for Van Mijenfjorden (Fig. 5.2.2).

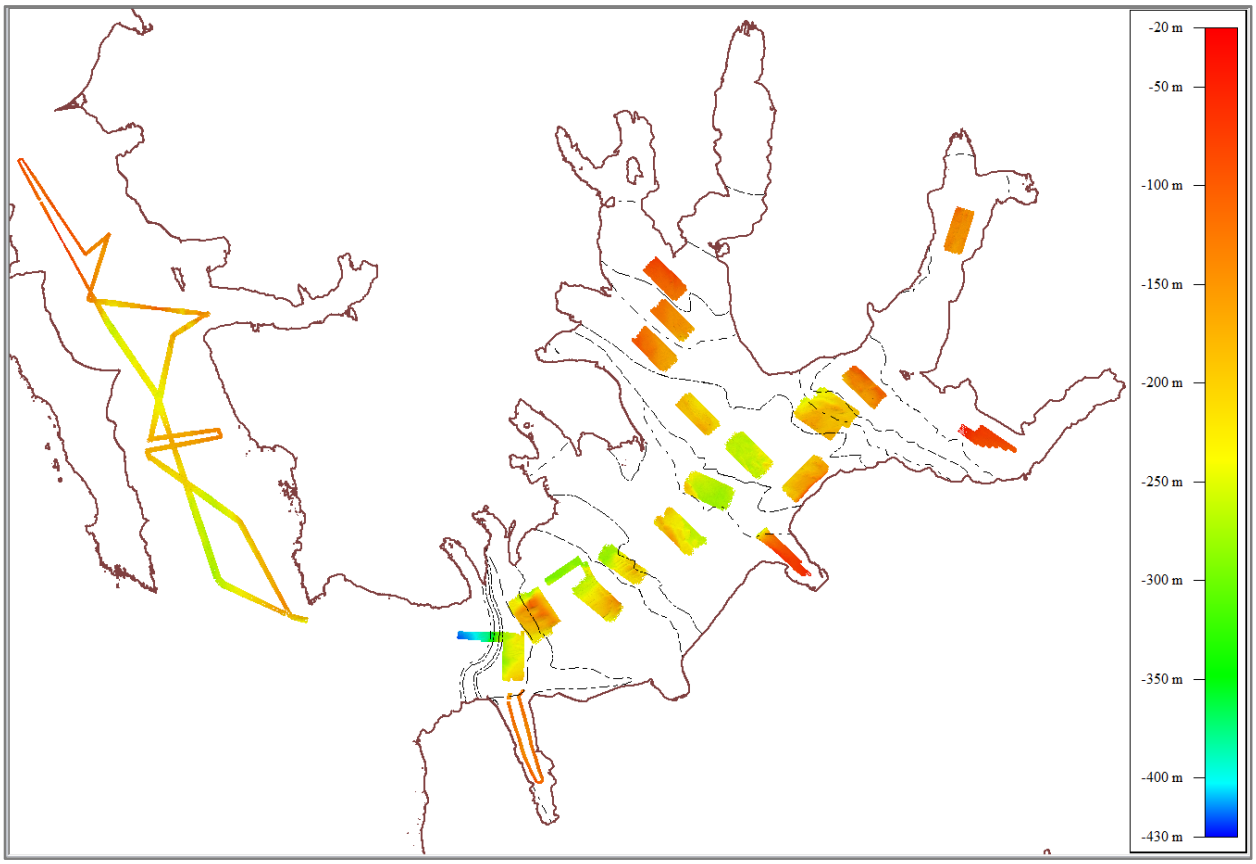

Fig. 5.2.1: Areas mapped with MBES in Isfjorden during the HE628 cruise. Dashed lines show boundaries of geological units.

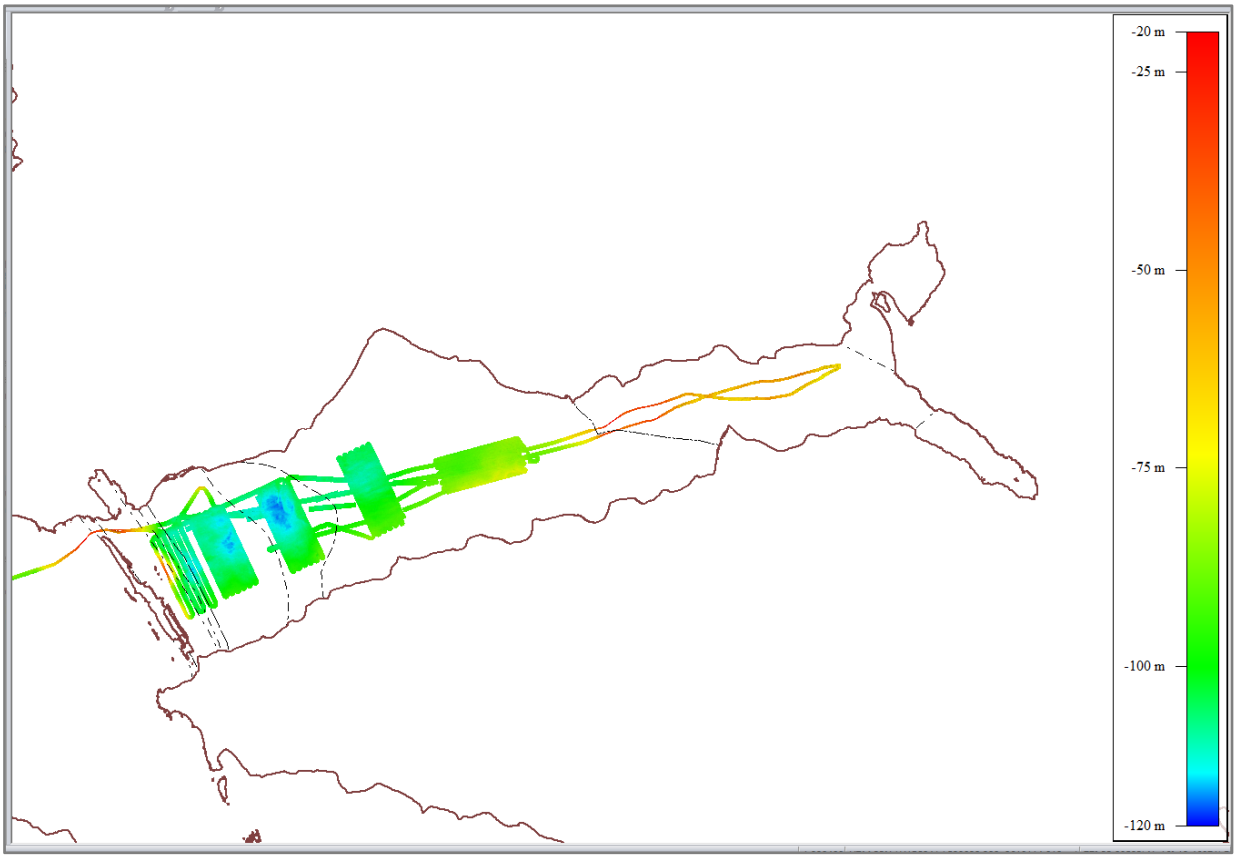

Fig. 5.2.2: Areas mapped with MBES in Van Mijenfjorden during the HE628 cruise. Dashed lines show boundaries of geological units.

5.3 Water Column Work by Multibeam

The main purposes of the surveys in the mapping boxes and transits between working areas were mapping for bathymetry (see chapter 5.2) and searching for gas flares in the water column. The Kongsberg Seafloor Information System (SIS) version 5.11.1 Build 447 was utilized for real-time visualization of the swaths and geo-picking of gas flares observed in the water column.

Preliminary Results

In Isfjorden, larger concentrations of flares were found over the Sassendalen Group, Kapp Toscana Formation, and Janusfjellet Subgroup. We also surveyed mapping boxes over the organic-rich units Agardhfjellet Formation (Middle Jurassic to Lower Cretaceous) and Botneheia Formation (Middle Triassic), which displayed very large concentrations of flares. Some clusters of flares appeared over Adventdalen Group and Van Mijenfjorden Group, displaying strong gas seepage close to the West Spitsbergen Fold and Thrust Belt (W of Isfjorden). Tempelfjorden and Gipsdalen groups did not show any signs of gas seepage. Similar results were found in Van Mijenfjorden and Van Keulenfjorden, with very few and weak flares appearing over Van Mijenfjorden and Adventdalen groups. There it highlights the presence of flares on the transects with outcropping Janusfjellet Subgroup. No gas flares were found in Kongsfjorden. On the continental slope west of Prins Karls Forland, a well-studied area where thousands of gas flares have been previously described (Gentz et al., 2014; Sahling et al., 2014; Mau et al., 2017), we found a large number of strong gas flares. Some of them were closely related to the observed oil slick.

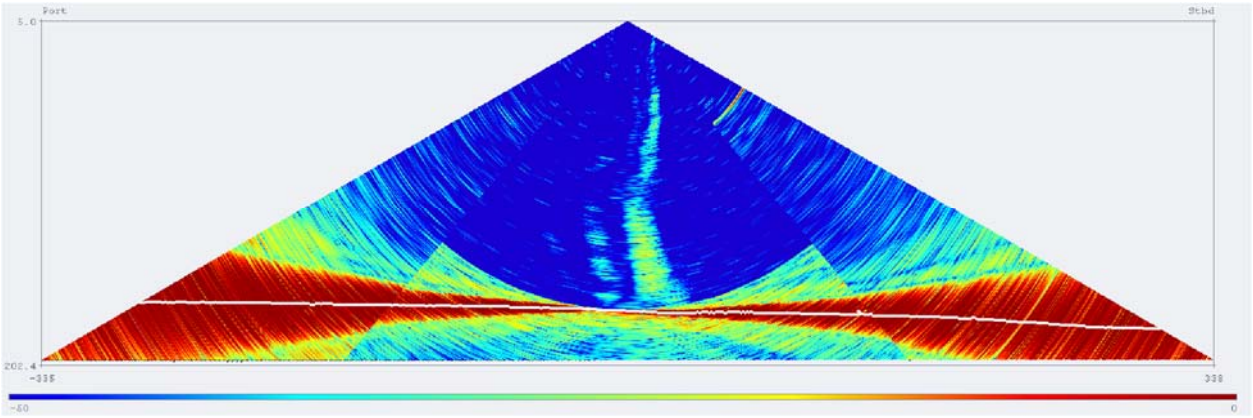

Fig. 5.3.1: At a depth of 171 meters, a pair of gas flares can be observed. The one on the right-hand side displays a steady gas flow that ascends to the water's surface. The left-hand side flare, on the other hand, operates differently by emitting gas in a pulsating manner, preventing it from reaching the water's surface.

5.4 Water Column Work by Fishechosounder

The Simrad EK60 scientific echo sounder system is designed for fishery research and has traditionally been used to locate fish resources and to measure stock abundance and size distribution. Recent research has shown that use of this echosounder not only improves fish stock assessment, but can be used as well for the detection and quantification of gas bubble emissions. A large number of transducers are available from Simrad, and we used a 38 kHz frequency transducer during HE628. The transducer is installed at the hull of the vessel and has an opening angle of 7°. ER60 is the real time operating software for the EK80. It displays the echogram, target position in the acoustic beam and target strength distribution.

Calibration

In order to maintain the accuracy provided by the Simrad EK80 and that is required for scientific applications, it must be calibrated. During calibration a reference target with known target strength is lowered into the sound beam, and the measured target strength is compared with the known target strength. If it is necessary to adjust the echo sounder, this is performed automatically by the calibration software. The reference target for the 38 kHz transducer is a copper sphere of 60.0 mm diameter with a known target strength of –33.6 dB. The ER60 has built in calibration software, which updates the system with accurate gain settings and beam pattern calculations. Calibration was performed on September 4th, 2023 before acquiring specific surveys to record data for flare detection and quantification. The copper sphere was lowered by three fishing gears below the hull of the vessel. In order to collect enough measurements in the beam sectors, the fishing lines were adjusted and additionally the vessels heading changed to move the sphere within the beam. Two calibrations were done for a pulse duration of 0.256 msec and 0.512 msec. The transmission power of 1000 W was used.

Preliminary results

Sites characterized by gas emissions and that has been selected for sampling were investigated in detail using dedicated EK80 surveys. The flares to be investigated have been crossed several times with different headings over a length of ~500 m each and with reduced vessel speed of ~3 kn, which finally resulted in a flower-like track geometry. These “EK80-Flowers” should allow for an

entire coverage of the gas emissions producing the flare or flares in its center. In total, 15 “EK80-Flowers” were conducted (including two repetitions). The raw data has a total size of 337 GB.

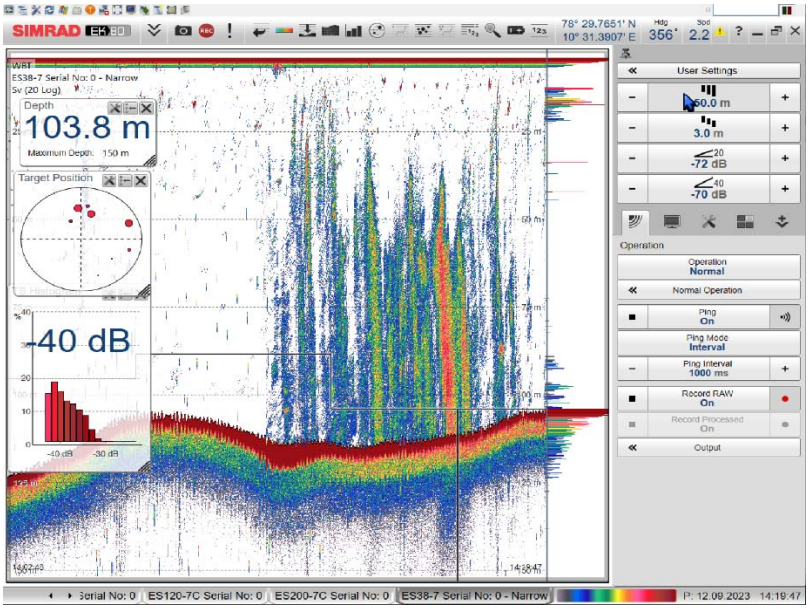

Fig. 5.4.1: Screenshot of an echogram recorded with EK80 during HE628. Gas bubble seepage from the seafloor become visible as flame-like anomalies of high backscatter into the water column.

5.5 Sub-bottom Profiling (SBP)

Data Acquisition

The INNOMAR SES2000 sediment echosounder system was used to image shallow sedimentary structures and gas anomalies down to a depth of ~40 m below seafloor. The SES 2000 employs the parametric effect to achieve a small signal opening angle at relatively low frequencies. The system sends out two primary high frequency signals at high energy levels. These primary frequencies interact in the water column to produce secondary frequencies (difference frequency) which travel within the small opening angle of the high frequencies. Thus, the parametric system has the advantage over conventional echosounders of a much-reduced footprint, resulting in increased lateral resolution of the system. Echosounder data was recorded for this cruise at a low frequency of 4 kHz with 1 pulse.

In total 36.3 GB of SES2000 data were recorded in 202 files (*.ses3) between 05/09/2023 06:54 and 24/09/2023 13:59. The *.ses3 data were further converted to SEGY format using the custom PS32SGY software (Hanno Keil, University of Bremen). The data were subsequently loaded into The Kingdom Software (IHS) for display and interpretation.

The echosounder was typically recording during transits between workstations. In addition, the SPB provided subsurface information along key cross- and in-lines across key workstations in Boxes 2, 4, 8, 11, 13, 17, 18, and 19. At these stations, SBP provided subbottom information supplementary to the large-scale EM712 and fine-scale EK80 mapping of selected flares.

Preliminary Results

The SBP’s main purpose was the detection of gas indications in sub-surface sediments, as well as to assess the rooting of geomorphological features. Typical gas indicators include acoustic blanking and/or enhanced reflectors (bright spots). Columnar blanking as well as narrow chimney-like features were detected in several profiles, most notably in the profiles taken during exploration cruising in Van Keulenfjorden. Other insights gained from the SBP included the occurrences of

well-layered sediments, that of chaotic deposits, and the lack of any consolidated sediments overlaying the bedrock. Chaotic signatures were most notable in close proximity to glacial forefields, where they were mostly interpreted as morphological features related to the presence of moraines. These secondary insights aided the suitability assessment to conduct gravity coring, an important secondary purpose of the SBP activity. In Fig. 5.5.1, a chimney structure with bright spots indicates the migration of gas from the subsurface into the water column. A local depression in the bathymetry is found directly above the columnar structure. A thin stratified overburden sits atop two packages of chaotic sediments that may represent glacial moraine infill and are delineated internally by a set of weak reflectors (~65 m bsl).

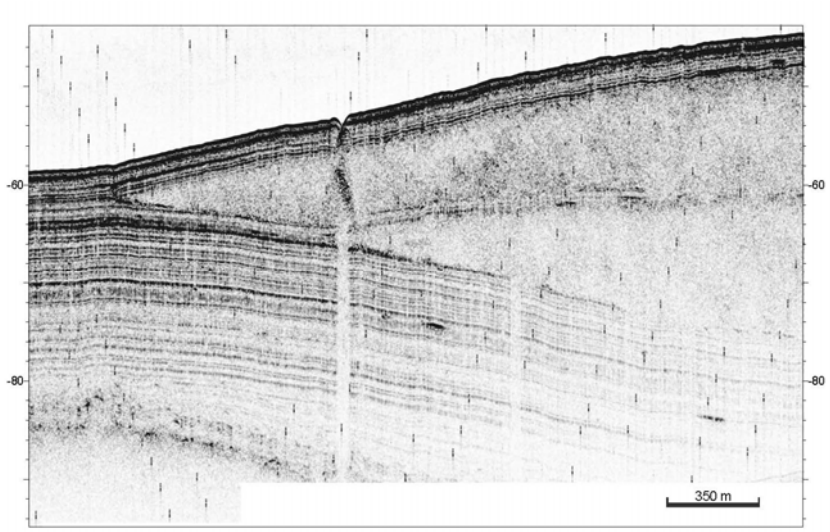

Fig. 5.5.1: Sub-bottom profile acquired during exploration cruising in Van Keulenfjorden.

5.6 MiniROV

Introduction and Methodology

The MiniROV is small low-cost remotely operated vehicle (ROV) developed by the Marine Environmental Research and Deep-Sea Engineering group at MARUM, University of Bremen. The MiniROV's mechanical hardware is mostly based on off-the-shelf prosumer grade products from Blue Robotics Inc. This includes the vehicle's frame, all pressure housing, buoyancy foam and most of the bulkhead penetrators, which connect different pressure housings. The MiniROV mechanical configuration is mainly based on the BlueROV2Heavy configuration offered off the shelf by blue robotics. This includes 8 BlueRobotics T200 thrusters, which enabled control of the MiniROV in all six degrees of freedom (6-DOF). In contrast to the commercially available BlueROVHeavy main electronic components such as the main processing unit (Raspberry Pi) were replaced by more capable commercial (Nvidia Jetson Nano) or custom-made alternatives. The MiniROV's software framework was based on the open-source robot middleware ROS2 Humble (Macenski, Foote, Gerkey, Lalancette, & William, 2022) and microROS (Belsare et. al, 2023) including custom written sensor interfaces and control architectures (Gutiérrez-Flores & Bachmayer, 2022). Due to its small size (46 x 58 x 25 cm), the deployment of the MiniROV can be simpler and more robust compared to classical commercial ROVs used in scientific expeditions. For shallow water operations the MiniROV can be deployed by one or two people from a small coaster or from the side of a research vessel (Römer et. al, 2021). BlueRobotics Inc. provides a neutrally buoyant unshielded tether (Fathom tether) of up to 300 m length to connect to the robot. Using two on-board packs of Li-Ion batteries the MiniROV can be deployed for several hours.

In contrast to previous deployments during the MSM98 cruise (Römer et. al, 2021) the MiniROV was outfitted with Aluminum pressure housings to enable dives at greater depths (target depths up to 300 m for this cruise). Several additional changes were needed to enable sampling up to 300 m depth. A garage was constructed to bring the MiniROV to target depth to save energy during launch and recovery (see Fig. 5.6.1). Additionally, a fiberoptic cable was used to facilitate better and more efficient data transfer between vehicle and the deck. The fiberoptic cable mounted on winch 3 of R/V HEINCKE was connected to a pressure housing mounted on the ROV garage, which contained a converter box and enabled the connection of the fiberoptic cable to the Fathom tether of the MiniROV, which was stored on the garage. The fathom tether in this application had a length of approximately 30 m. which enabled ROV operations up to 300 m depth with a 30 m search radius starting from the garage. A 300 m long standalone fiberoptic cable was kept as a fallback option in case of malfunction or connection issues to the ship's fiberoptics.

To sample gas directly at the seep sites in hundreds of meters depth, the simple gas sampling bags used for shallow water sampling during the MSM98 cruise (Römer et. al, 2021) were replaced by two small gas samplers designed for target pressures up to 30 bar. Each sampler consisted of a small titanium tank (approx. 15 ml sampling volume), a plastic funnel, a solenoid valve which could be controlled by the MiniROV, a needle valve to release the gas in a controlled manner on deck after sampling, buoyancy foam to neutralize the weight in water and a mechanical attachment to the MiniROV frame. To identify gas emissions, the MiniROV was equipped with a low light HD USB camera from Blue Robotics Inc. and four Lumen Subsea Lights (1500 lumen max) from Blue Robotics Inc.

Fig. 5.6.2: ROV garage with MiniROV inside.

For navigation purposes the MiniROV was equipped with a low-cost MEMS IMU (BNO-085 from Bosch), a pressure sensor (Bar100 High Resolution from Blue Robotics Inc.), a small DVL (A50 from WaterLinked) and a small USBL Transponder (Nano beacon from Sonardyne). Due to incompatibility issues between the native GAPS system from R/V HEINCKE and the Nano beacon

employed on the robot, a Sonardyne MicroRanger USBL transceiver was installed to facilitate georeferenced positioning.

MiniROV deployments

In total 4 stations were conducted with the MiniROV (see Table 5.6.1). Two out of those for constituted various tests to verify the working condition of the vehicle (station 10 and station 45), while the other two stations (12 and 25) were several hour-long deployments with live video feeds.

Table 5.6.1: List of MiniROV stations with relevant data.

Station Nr.	Mapping Box	Location		Depth [m]	Start time [UTC]	End Time [UTC]	Comments
		North	East				
10	1	78°19.887	15°40.474	96	-	15:15	Dry test
12	4	78°29.267	14°46.083	120	06:35	09:25	Microbial mats seen; no gas emissions
25	8	78°15.033	14°39.336	220	11:40	14:25	Carbonates and microbial mats seen; no gas emissions; termination due to issues with the vehicle
45	-	78°15.472	15°18.954	209	11:21	13:54	Pressure test

MiniROV Dive 1 (Station 12)

The MiniROV was deployed in mapping box 4 with a target depth of 120 m. The vehicle was connected to the deck by the ship's fiberoptic cable mounted on winch three. Deployment with the new garage went well and the MiniROV was successfully deployed to the target depth of 120 m. Driving out of the garage also posted no problem. However, due to some problems with the cable management the initial search radius for gas emission detection and sampling was limited to around 10 m. With progressing time, the issue could be solved so that in the latter half of the dive the full 30 m search radius was available. Visibility during deployment was limited due to a high density of zooplankton (likely a form of Chaetognatha**)**. During 2 h 25 min of time on the seafloor no methane emissions were spotted. However, several small microbial mats, indicating methane emissions, were found. When the batteries neared depletion the MiniROV was driven back into the garage for recovery, which was possible without problem.

From a technical perspective we could conclude from the first dive, that the new launch and recovery system, as well as the fiberoptic data connection worked well. In terms of scientific outcomes, indicators for methane emissions were found but no outgassing. Due to the high turbidity of the water during the dive, the recorded videos were analysed later on deck, but also in postprocessing no methane emissions could be detected in the field of view of the MiniROV's camera.

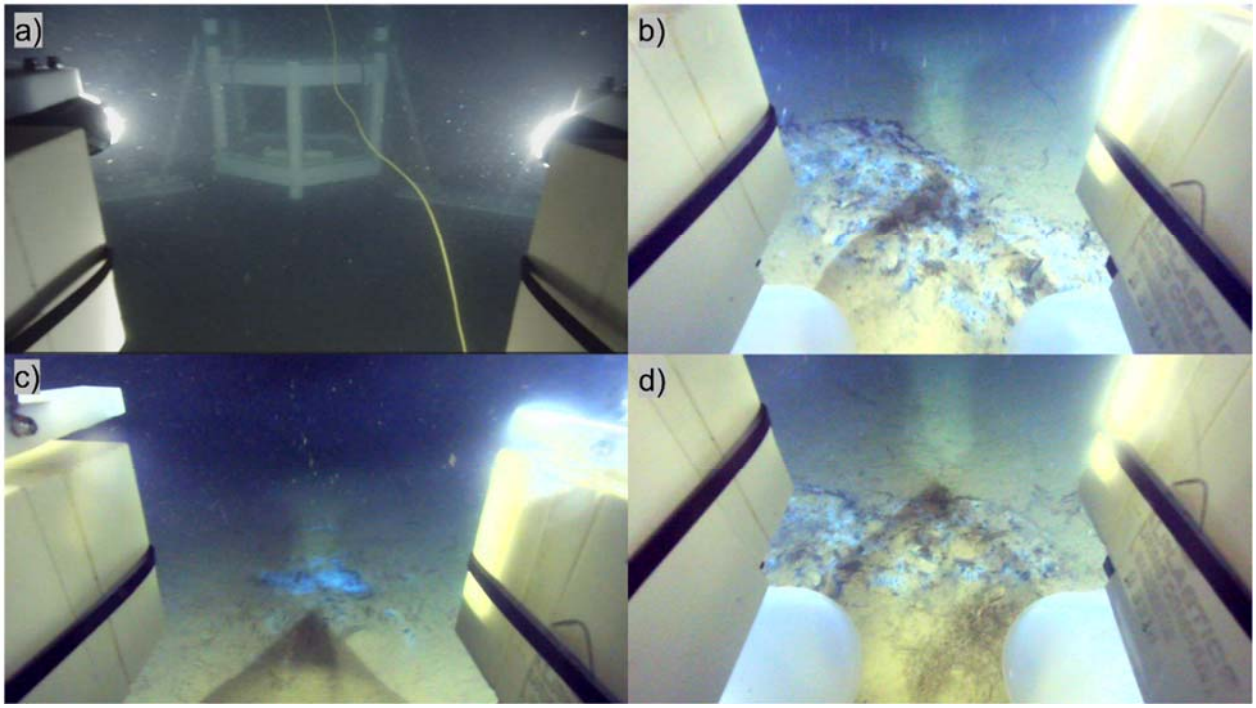

Fig. 5.6.3: a) view of the ROV garage from MiniROV camera after successful deployment and exit of garage. b) - d) detected microbial mats.

MiniROV Dive 2 (Station 25)

The MiniROV was deployed in mapping box 8 at a target depth of 220 m. Due to problems with the fiberoptic cable from winch 3, the backup standalone fiberoptic cable was used, which increased complexity of the deployment and recovery, which was handled very well by the deck crew. Deployment to the seafloor was conducted without problems. Similar to the first dive, some tether management issues restricted the available search radius for the MiniROV to 10 m. The tether management on the garage is therefore a design aspect needing some improvement in the future. Visibility for this dive was even more limited compared to the first dive, due to a high density of krill. The krill specifically clustered around the MiniROV's lights when the robot was hovering in place. This made the visual in-situ search for gas bubbles challenging. Again, during the 2h 18min of search on the seafloor no gas emissions could be identified. Neither could any emissions be seen while postprocessing the video on deck afterwards. However, several bacterial mats and carbonated crusts were found, indicating a close proximity to the targeted emission site (see Figure 5.6.3). In the last minutes of the 2h 18 min lasting dive, commination problems between deck and MiniROV occurred, which led to the abortion of the dive. Fault diagnosis on deck revealed that one of the pressure housings was compromised, which lead to a significant leak and severe problems with the low-level motor control and sensor interface electronics. Further pressure tests (MiniROV deployment 4 / station 45) with new sealing components showed a significant improvement but still minor leakages after 2h at 200 m depth. Due to time constraints related to further necessary testing for fault detection and availability issues regarding spare parts no further MiniROV dives could be conducted afterwards.

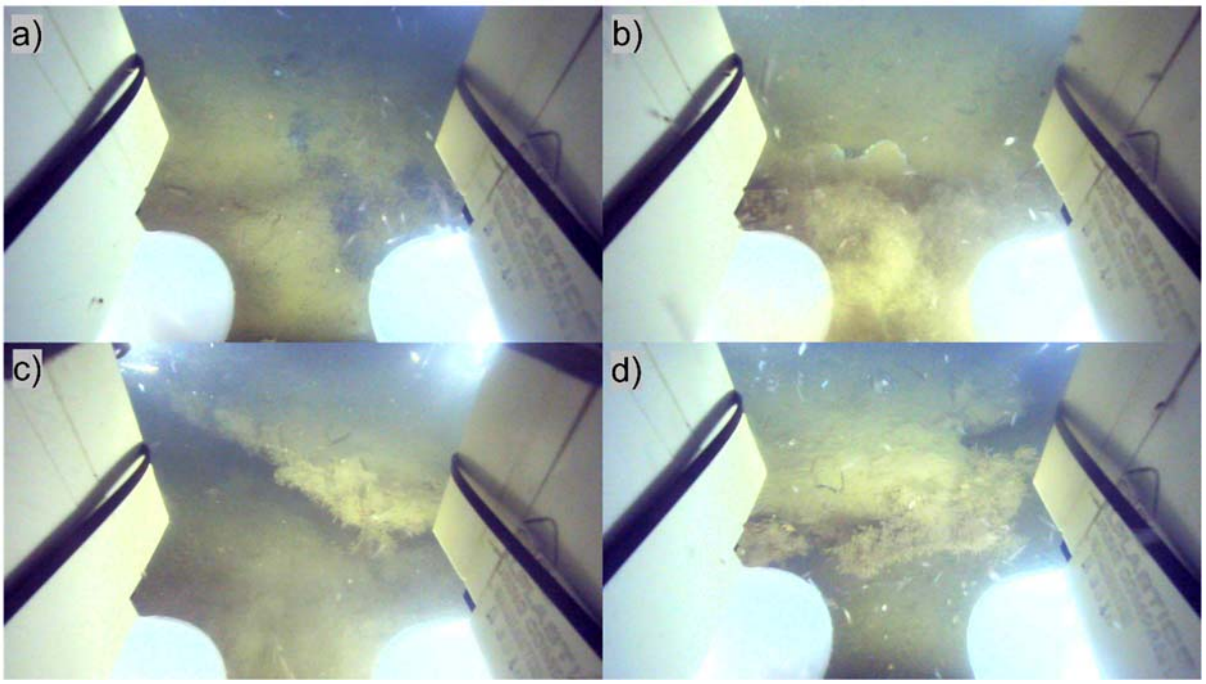

Fig. 5.6.4: a) detected microbial mats, b) - d) detected carbonated crust

5.7 Hydrography and Distribution of Dissolved Methane in the Water Column

Introduction

The spatial distribution of methane, which is emitted into the water column in the form of gas bubbles and causes hydroacoustic anomalies (flares), is of great importance with regard to its fate in the water column and potential transfer into the atmosphere. During expedition HE628, CTD/Ro (conductivity, temperature, density/ Rosette water sampler) stations were conducted in the different fjord systems in high flare density areas in order to record continuous vertical hydrographic and to determine concentrations of dissolved methane in discrete water samples.

Methods

During HE628 a CTD/Ro-system that is permanently installed on R/V HEINCKE and maintained by the Physical Oceanography group of AWI (Bremerhaven) was used. The set of sensors mounted to the frame of the CTD/Ro-system was comprised of a Sea-Bird SBE 9 instrument package with paired standard modular temperature and conductivity sensors and a pressure sensor. Auxiliary sensors integrated with the CTD were two Sea Bird Scientific SBE 43 Dissolved Oxygen Sensors, a WET Labs ECO-AFL/FL Fluorometer, a WET Labs C-Star Transmissometer, and an Altimeter. For the objectives of expedition HE628, the data from the fluorometer were of minor interest and were therefore not evaluated.

For sampling of discrete water samples in selected water depths, twelve 5-L Niskin bottles attached to the rosette were closed during heaving of the CTD/Ro system. Water sampling from the Niskin bottles and analysis for concentrations of dissolved methane was done according to a method reported by Mau et al. 2020. Briefly, 100 ml of water was filled from each Niskin bottle into tow 140 ml plastic syringes using a silicone tube making sure that no air bubbles remained in the syringes. 40 ml of methane-free synthetic air were added to each of the syringes and the syringes were shaken vigorously for >1.5 minutes to allow for equilibration between water and

headspace. The 40 ml headspace gas of each of the two syringes was transferred in another dry 140 ml syringe.

Concentrations of dissolved methane in the headspace gas extracted from discrete water samples were determined on board with a Greenhouse Gas Analyzer (GGA, Los Gatos Research) (Mau et al. 2020). The 80 ml of headspace gas (40 ml of each of the sampled syringes) was injected in the GGA. This was immediately followed by injection of 60 ml of synthetic air, as needed to reach the required volume of 140 ml of the analyzing chamber of the GGA. The reproducibility of the method is <2.5%.

Preliminary results

In total 21 CTD/Ro stations located in 16 different areas (resp. 15 of the defined boxes) were conducted successfully during HE628 (Table 5.7.1). An exemplary T-S diagram is shown in Fig. 5.7.1 for the Isfjorden, where thirteen of the CTD/Ro stations were carried out.

Table 5.7.1: List of CTD/Ro stations carried out during cruise HE628.

Ship Station No.	Instrument Deployment No.	Area (Fjord)	Box	Water Depth (m)
004	CTD-1	Isfjorden	Box 2	272
009	CTD-2	Isfjorden	Box 1	98
013	CTD-3	Nordfjorden	Box 4	120
019	CTD-4	Isfjorden	Box 8	223
029	CTD-5	Isfjorden	Box 12	289
030	CTD-6	Isfjorden	Box 11	187
033	CTD-7	Prins Karls Forlandet		114
037	CTD-8	Prins Karls Forlandet		112
038	CTD-9	Isfjorden	Box 13	171
050	CTD-10	Van Mijenfjorden	Box 17	111
054	CTD-11	Van Mijenfjorden	Box 18	106
057	CTD-12	Van Mijenfjorden	Box 19	83
062	CTD-13	Isfjorden	Box 8	222
064	CTD-14	Isfjorden	Box 7	223
065	CTD-15	Billefjorden	Box 23	163
067	CTD-16	Isfjorden	Box 2	268
069	CTD-17	Nordfjorden	Box 24	174
070	CTD-18	Isfjorden	Box 2	272
072	CTD-19	Isfjorden	Box 15	424
073	CTD-20	Isfjorden	Box 15	423
075	CTD-21	Isfjorden	Box 3	259

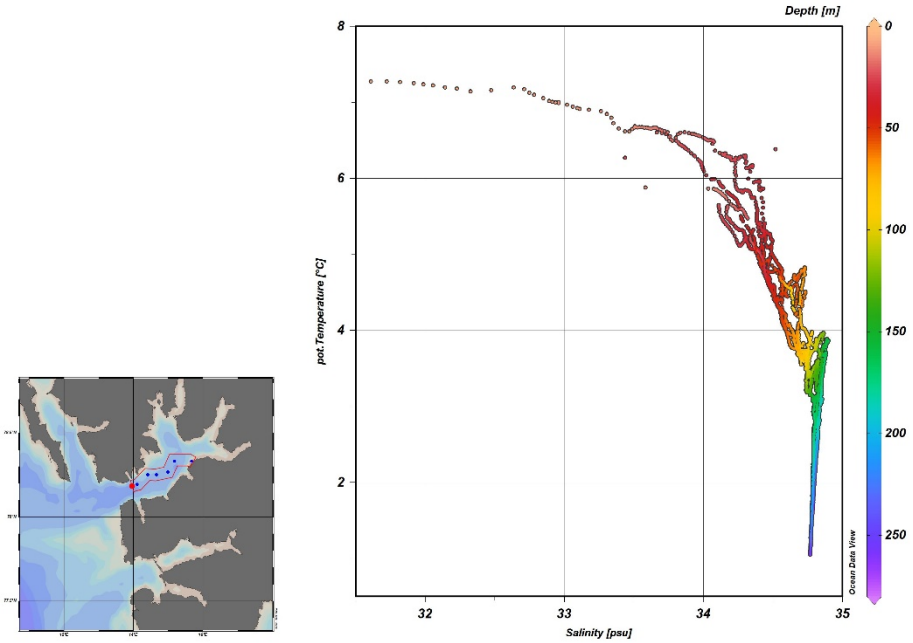

Fig. 5.7.1: Potential Temperature-Salinity (T-S) plot of all the CTD data collected in Isfjorden during HE628. Colour bar indicates water depth.

During the time of investigation in September 2023, the water column in Isfjorden was characterized by at least two water masses. While the water mass below approx. 130–150 m was characterized by relatively constant salinities around 34.7 and a temperature range of approx. 0.7 - 3.9 °C, lower salinities (approx. 31.5–34.7) and higher temperatures (3.9–7.3 °C) were detected in the overlying water body.

Dissolved methane concentration was determined for 252 discrete water samples collected at all CTD/Ro station during HE628. In general, concentrations at most stations ranged between 7.0 and 27.5 nmol/L in the uppermost 5 to 50 m (see Fig. 5.7.2 left), except for the two stations conducted at the western continental margin west off Prins-Karls-Forlandet (CTD-7, -8) where slightly higher concentrations around 50 nmol/L were recorded at water depths of around 50 m (see Fig. 5.7.2 right). At all stations enrichments in methane were observed in the deeper water body, and highest concentrations (~370 nmol/L) were found at station CTD-08 off Prins-Karl-Forlandet ~34 m above ground (Fig. 5.7.2 right). Within the fjord systems investigated maximum concentrations of ~84 nmol/L were detected at station CTD-9 at the transition from the southwestern Isfjorden to the open sea (Box 13) ~15 m above ground. Initial results suggest that gas bubble release identified as hydroacoustic anomalies (‘flares’) does not lead to spatially limited methane concentration anomalies in the tens to hundreds of meters range in the middle and upper water column, but rather to a wide distribution throughout the water body.

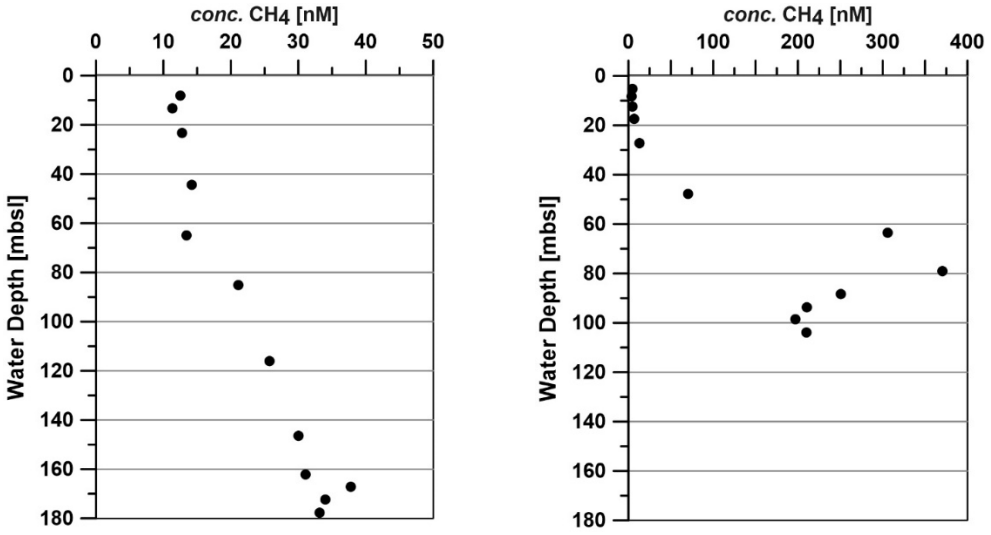

Fig. 5.7.2: Exemplary vertical profiles of dissolved methane concentrations in discrete water samples collected at station CTD-6 at the southwestern part of Isfjorden (Box 11) (left) and station CTD-8 west off Prins-Karls-Forlandet (right).

At the two stations on the continental shelf off Prins-Karls-Forlandet (CTD-7, -8) enrichments of methane in the water column, maximizing approximately ~33 m above seafloor was observed (Fig. 5.7.2, right). The vertical distribution of dissolved methane at these sites resembles that previously described for a region ~30 km northwest, located on the continental slope at an average water depth of 245 m (Gentz et al., 2014). In that region enrichments of methane of up to ca. 520 nmol/L in summer 2010 (cruise HE333) were related to efficient trapping below a salinity-controlled pycnocline ~20 m above the seafloor, which hampers vertical diffusive transport and sustains lateral transport of dissolved methane in the same density layer. Joint analysis of all hydrographic and methane-related data obtained during HE628 will show whether the methane enrichments observed at the shallower stations on the Continental Shelf can also be attributed to this process.

5.8 Sediment Sampling and Analysis

Introduction

Sediment cores were taken to investigate the lithological composition and geochemical properties of near-seafloor sediments in areas that are affected by hydrocarbon seepage as discovered during hydroacoustic surveys in the various fjord systems (see Fig. 5.8.1). For instance, the relative strength of the methane flux from below can be assessed based on the depth of the sulfate-methane interface (SMI) (Borowski et al., 1996).

Sampling

During cruise HE628 gravity cores (GC) up to 541 cm in length were collected for the analysis of deep sediments (Table 5.8.1), whereas up to ~50 cm-long cores of undisturbed seabed sediments were taken with a multicorer device (MUC) (Table 5.8.2).

Table 5.8.1: List of gravity cores collected during cruise HE628.

Ship Station No.	Instrument Deployment No.	Core Identifier (GeoBxx)	Area (Fjord)	Box	Cored Length [cm]
006	GC-1	25606-1	Isfjorden	Box 2	66
008	GC-2	25608-1	Isfjorden	Box 2	254
014	GC-3	25614-1	Nordfjorden	Box 4	258
017	GC-4	25617-1	Isfjorden	Box 2	541
020	GC-5	25620-1	Isfjorden	Box 8	455
021	GC-6	25621-1	Isfjorden	Box 2	38
022	GC-7	25622-1	Isfjorden	Box 2	few cm *
031	GC-8	25631-1	Isfjorden	Box 11	272
034	GC-9	25634-1	W‘ of Prins Karls Forlandet	n.a.	40
035	GC-10	25635-1	W‘ of Prins Karls Forlandet	n.a.	270
040	GC-11	25640-1	Isfjorden	Box 13	217
041	GC-12	25641-1	Isfjorden	Box 13	few cm *
051	GC-13	25651-1	Van Mijenfjorden	Box 17	371
056	GC-14	25656-1	Van Mijenfjorden	Box 18	431
059	GC-15	25659-1	Van Mijenfjorden	Box 19	359
068	GC-16	25668-1	Isfjorden	Box 2	539
071	GC-17	25671-1	Isfjorden	Box 2	367
				Total	**~4,478**

n.a. – not assigned, bulk sample stored in plastic bag

Table 5.8.2: List of multicorer stations conducted during cruise HE628.

Ship Station No.	Instrument deployment No.	Core identifier (GeoBxx)	Area (Fjord)	Box	No. of cores filled with sediment
005	MUC-1	25605-1	Isfjorden	Box 2	3/4
026	MUC-2	25626-1	Isfjorden	Box 8	4/4
039	MUC-3	25639-1	Isfjorden	Box 13	1/4
042	MUC-4	25642-1	Isfjorden	Box 13	3/4
044	MUC-5	25644-1	Nordfjorden	Box 4	3/4
046	MUC-6	25646-1	Isfjorden	Box 2	3/4
052	MUC-7	25652-1	Van Mijenfjorden	Box 17	4/4
055	MUC-8	25655-1	Van Mijenfjorden	Box 18	3/4
058	MUC-9	25658-1	Van Mijenfjorden	Box 19	3/4
066	MUC-10	25666-1	Billefjorden	Box 23	3/4
079	MUC-11	25679-1	Adventfjorden		none
080	MUC-11	25680-1	Adventfjorden		3/4

Sediment gravity cores were collected with a gravity corer from MARUM - Center for Marine Environmental Sciences, University of Bremen, which was equipped with a head weight of around ~600 kg and a 5.75-m (occasionally 3-m) core barrel. Underwater navigation was achieved with the GAPS positioning system installed on R/V HEINCKE, and the transponder was attached to

the wire about 20 m above the weight. Lowering speed and seafloor penetration speed were usually 0.5 m/s (max. 0.7 m/s). In total 17 gravity corer stations located in 9 different areas (resp. 8 of the defined boxes) were conducted during cruise HE628, and sediments were retrieved at all stations (Table 5.8.1).

Immediately after recovery, the plastic liner (12 cm ID) inside the core barrel was cut into 1 m-long segments on deck. Sediment samples (3 mL) for headspace analysis of concentrations of dissolved hydrocarbons and methane stable carbon and hydrogen isotopic compositions were taken with 5-ml cut-off plastic syringes from the fresh cuts. The samples were transferred into 20-mL crimp vials, which were sealed with silicone/PTFE crimp caps. The core segments were taken to the wet lab, where the sediment was made accessible through openings (about 2 x 3 cm) sawn into the liner at specified intervals (in most cases 25 cm). Additional samples for the analysis of dissolved hydrocarbons (methane) and samples for the analysis of sediment porosity as well as bulk contents of inorganic and organic carbon and total nitrogen (e.g., C_{org}/N_{tot}) were taken with cut-off plastic syringes (3 to 5 ml of sediment each) (Table 5.8.3). Subsequently, rhizon fluid samplers were introduced into the sediment and pore water was extracted by applying a vacuum with a 10-mL plastic syringe. Immediately after sampling, pore waters were separated into four aliquots for analysis of major anions using ion chromatography, of elements using inductively coupled plasma optical emission spectrometry, as well as for dissolved inorganic carbon and non-purgeable organic carbon with a carbon analyzer in the home lab. After sampling the liners were closed again with the cut-out pieces of the liner and tape. The whole-round segments of the gravity cores were stored at 4°C in the cooling room of R/V HEINCKE.

Table 5.8.3: List of sediment samples taken for the various types of analysis in the home lab.

Target	**Gravity Cores**	**MUC cores**
Headspace gas, concentrations CH_4	222	121
Headspace gas, stable C and H isotopic comp. CH_4	481	
Porewater	170	
Porosity, C_{org}/N_{tot}	221	112
Micropaleontology		155
Ancient DNA		495

Multiple sediment cores comprising the seabed-bottom water interface were collected at locations from which gravity cores had already been collected. For this, a MUC device provided by the Marine Geochemistry group of the Alfred Wegener Institute, Helmholtz Centre for Polar and Marine Research, Bremerhaven (AWI) was used. Typically, four plastic tubes (62 cm length, 9.2 cm ID) were installed in the MUC device before deployment. The transponder was placed 50 cm above the frame of the MUC. During deployment the device was placed on the seabed at a speed of ~0.1 - 0.2 m/s. In total 11 MUC stations located in 9 different areas (resp. 8 of the defined boxes) were conducted during cruise HE628. At two stations only less than two tubes filled with sediment were recovered (Table 5.8.2).

Immediately after recovery on deck, two tubes were used to sample sediments for the analysis of methane concentrations in headspace samples (usual distance 2 – 5 cm each) as well as sediment porosity and bulk contents of inorganic and organic carbon and nitrogen (C_{org}/N_{tot}) as described above. A third core was used to isolate sediments for sedimentary DNA analysis and micropaleontological investigations. Samples for DNA analysis were taken from cores retrieved

during the ten successful stations (length between 18 and 46 cm) in order to investigate the vertical gradient of sedimentary DNA burial and to understand how the ancient DNA archive is formed. In order to avoid contamination, sediment sampling was carried out on deck at –1 to 4°C air temperature as follows: The surface sediment was sampled with a sterile (5% sodium hypochlorite and 70% ethanol solutions) spatula and isolated into a 2 mL Eppendorf tube in three replicates. Further 2 cm of the core were extruded, and the sediment was then lifted and flipped with a spatula on itself to expose the inner part of the core. The sediments were sampled in the inner part of the core and isolated into 2 mL Eppendorf tubes in three replicates. The remaining extruded sediments were recovered into a sampling bag for micro-paleontological analyses. The same procedure was repeated until the bottom of the core was reached. The sediment samples isolated for DNA analyses were wrapped with parafilm and frozen at –50°C on board. Samples, obtained for micro-paleontological analyses, were stored at 4°C. For most stations, a single core was additionally stored at -50°C in a freezer onboard R/V HEINCKE for analysis of biomarkers in the home lab.

The cooled gravity core segments and frozen MUC cores were transported to the University of Bremen Upon arrival of R/V HEINCKE in the port of Bremerhaven after cruise HE629. The gravity core segments will be cut lengthwise, separated into a working half and an archive half, photographed with the GeoB smart-CIS 1600 Line Scanner, and described macroscopically. Subsequently, the cores will be stored in the MARUM GeoB Core Repository, where they will be accessible upon request.

Analysis

Methane concentrations in headspace samples were determined onboard with an Agilent Technologies, 7890B gas chromatograph equipped with a flame ionization detector (Pape et al. 2020). Sediment porosity as well as bulk contents of inorganic and organic carbon and nitrogen will be analyzed in the lab of the 'General Geology – Marine Geology' group at MARUM/Faculty of Geoscience at the University of Bremen (Pape et al. 2020). Stable carbon and hydrogen isotopic compositions of pore water dissolved methane sampled from gravity cores and MUC cores will be determined in the MARUM Stable Isotope Laboratory. Concentrations of indicative pore water ingredients (e.g., Cl^-, SO_4^{2-}, Ba^{2+}) will be analyzed in the lab of the Sediment Geochemistry group at MARUM.

Preliminary results

Analysis of samples from gravity cores and MUC cores demonstrated methane enrichments a few decimeters to meters below the seafloor at all sites investigated. Most gravity cores penetrated the SMI, where the microbially-mediated anaerobic oxidation of methane (AOM) takes place, in depths greater than one meter. As a consequence, strong depletions in methane concentrations were usually observed in uppermost sediments recovered with gravity cores and MUC cores (Fig. 5.8.1 left). However, for MUC cores from station MUC-6 conducted in Isfjorden, Box 2, intense migration of free gas bubbles through the core and escape from its top was observed. Furthermore, maximum methane concentrations below the SMI were of the same order of magnitude in both cores (GC-16: ~480 µmol/L; MUC-06: ~670 µmol/L). This suggests that significant amounts of upwardly migrating methane can bypass the AOM zone, which at this site is positioned only a few centimeters below the seafloor (Fig. 5.8.1 right). Furthermore, the very different depths of the SMI in GC-16 (approx. 360 cm) and MUC-06 (approx. 3 cm) indicate the occurrence of localized, near-surface methane enrichments in this part of the Isfjorden.

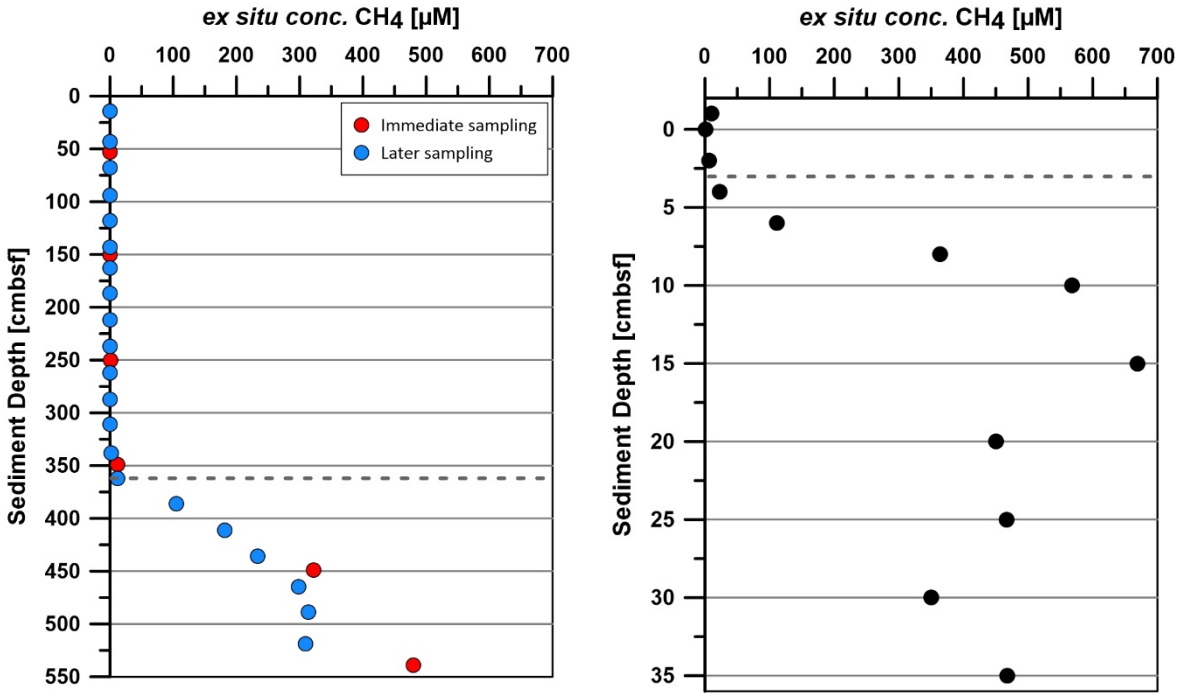

Fig. 5.8.1: Exemplary vertical concentration profile of dissolved methane in gravity core 16 (left) and MUC core 06 (right) taken nearby in the Isfjorden, Box 2. The horizontal stippled line illustrates the assumed depth of the SMI. Samples below ~450 cm in GC-16 and below ~10 cm in MUC-06 show reduced methane concentrations due to ongoing degassing at atmospheric pressure.

Future work will focus on a joint evaluation of lithological and (isotope) geochemical data from all sediment cores for a comprehensive characterization of the hydrocarbon affected locations in the western fjords of Spitsbergen.

5.9 Continuous Air Measurements With the Greenhouse Gas Analyzer ICOS

System overview

A greenhouse gas analyzer manufactured by Los Gatos Research (LGR) was used to determine CH_4 and CO_2 concentrations continuously during HE628. This instrument, called Integrated Cavity Output Spectroscopy (ICOS), uses conventional laser absorption spectroscopy, where the absorption of the infrared laser beam directed through the sample is used to calculate the mole fraction of methane in the gas. The ICOS was installed in the beginning of the cruise in the wetlab on the R/V HEINCKE and was calibrated with standard gases within the range of 0 ppm to 10 ppm. During the period of scientific program, precision of the instrument was checked daily with 1 and 10 ppm methane standard.

The main use of the ICOS during this cruise was the continuous methane concentrations monitoring above the sea level. Using the Tygon hoses, the ambient air was sucked in via a pump and transferred into the analysis device. In order to achieve the best possible results, and to avoid any water getting into the ICOS instrument chamber at the same time, especially during rough weather, the end of the Tygon hoses was installed as close as possible, but as high as necessary above the sea level. The aim of this technique is to detect methane gas emissions from the flares in the atmosphere.

Preliminary results

Measurements were taken continuously throughout the entire cruise. They were interrupted only during the measurements for the CTD water samples. Besides that, the ICOS ran continuously for 24 hours at a rate of 1Hz. Figure 1.1 shows the overview of the ships track and represents the entire course of the measurements. Background measurements for methane in the air are typically between 1.95 and 1.99 ppm. Peaks of elevated methane concentrations occurred numerous times (see example in Fig. 5.9.1), however, careful analyses in the home lab are needed to evaluate their sources. The maximum value reached was 2.34 ppm when passing over the oil bubble release offshore Prins Karls Forlanded.

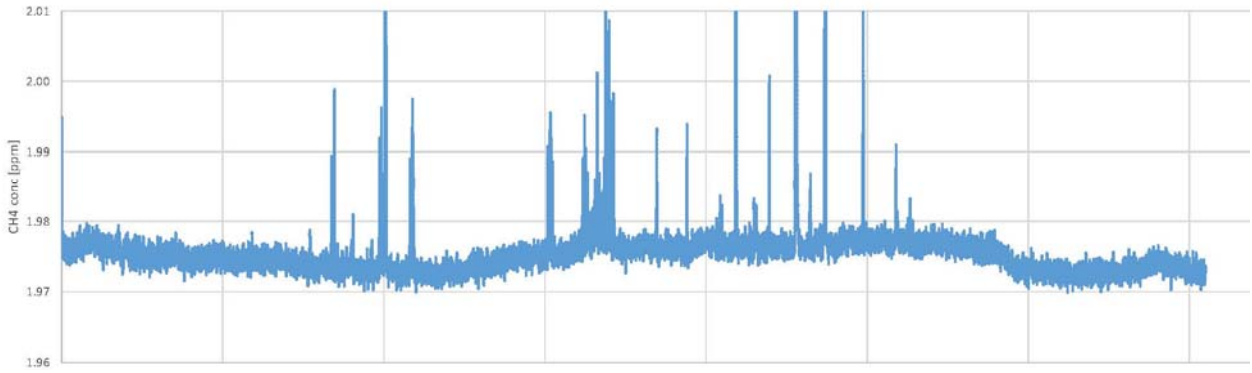

Fig. 5.9.1 Preliminary results of the continuous methane measurements during HE628. Exmple of a time series of around one day. Background values are around 1.97 to 1.98 ppm during this day, while clear peaks with values >1.99 ppm occurred when crossing a seep area several times.

5.10 Sonar Lander

The sonar lander (Fig. 5.10.1) is an autonomous, battery-powered instrument designed to monitor the variations of methane gas emissions from the seabed over several days. The sonar lander consists of a single-beam scanning-sonar (IMAGENEX 881A, 675 kHz) mounted on a 220 x 220 cm galvanized steel frame. The sonar is operated by a control module located inside a pressure housing. Power is supplied by two 24V oil-filled DSPL battery packs (2x38 Ah). The frame has a low height (< 70 cm) and a trapezoidal shape making it less at risk of damage in case of trawling activities in the area of deployment. Because of the low-height of the instrument, the scanning-sonar was tilted at a 41° angle relative to the horizontal plane to prevent any undesired backscatter caused by the seafloor or by the lander frame, thus facilitating the detection of gas bubbles in the water column. The sonar detection range was set to 10 m with a gain setting of 20 dB, a scanning sector of 180°, and a step size of 0.3°. A CTD probe (Sea&Sun Technology CTD48M memory probe) fixed onto the lander provided timeseries of in-situ environmental parameters (salinity, temperature, pressure) for the duration of the sonar lander deployments. Additionally, we mounted a forward-looking PlasPI camera (Purser et al., 2020) onto the lander frame to provide "groundtruthing" photos and videos in order to facilitate the interpretation of the sonar data. The PlasPI is a self-contained battery-powered time-lapse underwater camera equipped with a Raspberry Pi NoIR Camera V2 and a LED lamp. The internal clocks of the sonar, the CTD probe and the PlasPI camera were set to UTC time and synchronized before each deployment.

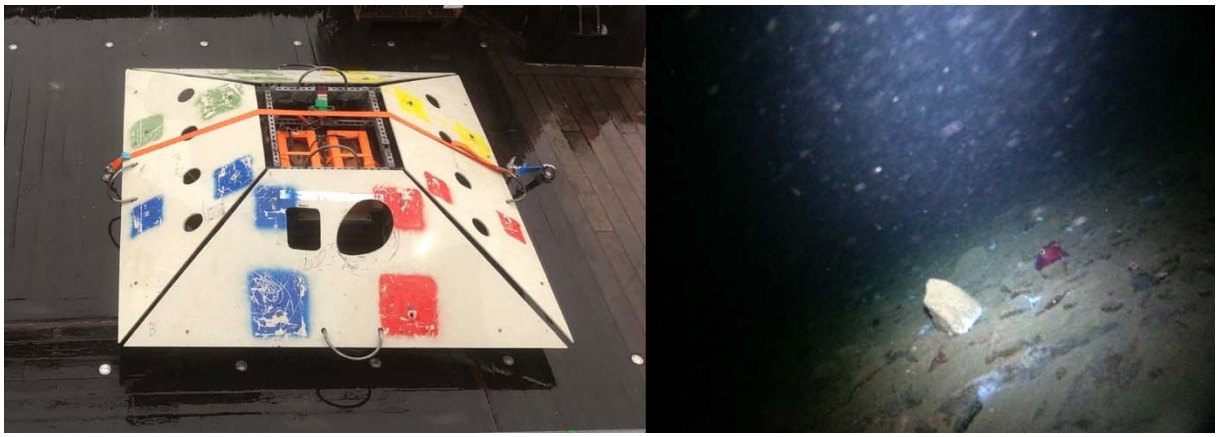

Fig. 5.10.5: The sonar lander (left). Right: PlasPI still acquired during deployment #3. Patches of white microbial mats are present on the seabed. Gas emissions are not visible due to the large amount of marine snow and limited visibility (right).

The sonar lander was deployed four times (Table 5.10.1) in the vicinity of known gas bubble emissions at water depths between 128 m and 229 m. Unfortunately, no sonar data were recorded during deployments #2 and #4 due to technical failures. In total, the sonar conducted 547 scanning sequences during deployment #1 and 1,143 scanning sequences during deployment #3 with an interval of 5 minutes between each sequence. Each scanning sequence lasts about 3 minutes and contains at least five complete scans of 180°.

Deployment #1 lasted about 2 days and targeted a site where several recurrent gas bubble streams occur. Unfortunately, no gas emissions could be detected within the sonar range. Deployment #3 lasted about 4 days and took place at the site of a strong persistent bubble plume. This deployment was successful, in that active bubble plumes are clearly visible on the sonar records (Fig. 5.10.2). Preliminary observations from this deployment showed that multiple gas emissions were present within the sonar range. The strongest emissions were continuously active over the entire deployment duration. Some of the weaker gas emissions displayed a more discontinuous behavior with short intervals of inactivity. In deployment #1, we mounted the PlasPI near the top of the lander's right-hand sideplate. However, the resulting images achieved extremely poor visibility due to large amount of marine snow in the area, which caused strong light backscattering. In order to optimize the visibility for deployment #3, we placed the camera nearer to the bottom of the right-hand sideplate, i.e. closer to the seabed. The camera ISO setting was set to 200 for images with artificial lighting and to 800 for images without artificial lighting. The PlasPI camera was not used for the deployments #2 and #4 because of the higher water depth, which exceeded the camera's depth rating. The camera images and videos showed patches of white microbial mats on the seabed but no gas emissions (Fig. 5.10.1). The visibility is strongly limited by dense marine snow. The sonar .81A binary files, the PlasPI footage, and the CTD data will be archived on the PANGAEA data repository

Table 5.10.2: Details of the sonar lander deployments during HE628.

	Deployment 1	**Deployment 2**	**Deployment 3**	**Deployment 4**
Station Numbers	16 (deployment) 24 (recovery)	28 (deployment) 43 (recovery)	48 (deployment) 61 (recovery)	63 (deployment) 74 (recovery)
Deployment location	Box 4	Box 8	Box 13	Box 8
Deployment coordinates	78°29.256' N 14°46.259' E	78°15.029' N 14°39.345' E	78°11.634' N 14°05.924' E	78°15.031' N 14°39.350' E
Deployment depth	128 m	229 m	174 m	228 m
Start of monitoring period	08.09.2023 09:30 UTC	11.09.2023 08:00 UTC	16.09.2023 07:30 UTC	20.09.2023 14:30 UTC (CTD)
End of monitoring period	10.09.2023 07:00 UTC (Sonar, CTD, PlasPI)	13.09.2023 14:30 UTC (CTD)	20.09.2023 06:35 UTC (Sonar, CTD) *18.09.2023 13:15 UTC (PlasPI)**	23.09.2023 13:15 UTC (CTD)
Acquisition schedule				
Sonar	every 5 minutes	No data recorded	every 5 minutes	No data recorded
CTD probe	every 15 sec	every 5 sec	every 30 sec	every 30 sec
PlasPI stills (with LED)	2x photos every 5 minutes		2x photos every 5 minutes	
PlasPI videos (with LED)	1x 10 second-video every hour		1x 10 second-video every hour	

** The PlasPI camera batteries ran out after about 2.5 days.*

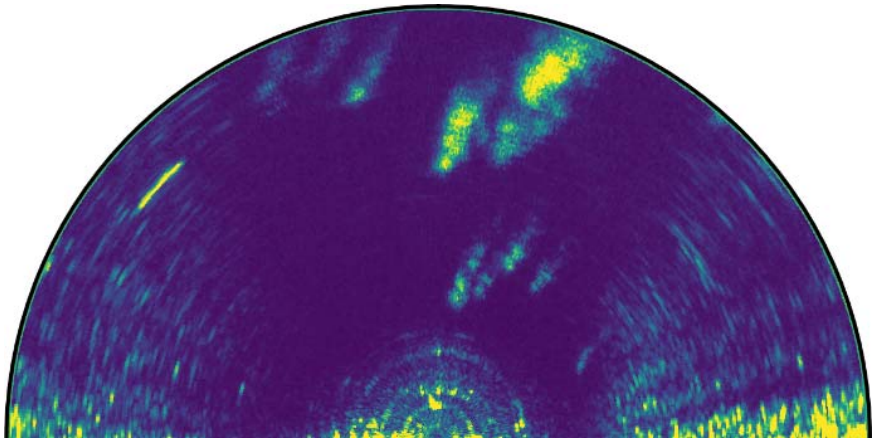

Fig. 5.10.2: Sonar scan recorded during deployment 3, showing strong anomalies caused by gas bubble emissions.

6 Station List

6.1 Station List

					Time (UTC)				Begin / on seafloor			
Date	Station	GeoB no.	Instrument	Location		on	off		Latitude	Longitude	Water	Core length/Penetration/Recovery
	HE628/				Begin	seafloor	seafloor	End	N	E	depth (m)	Remarks
04/09/2023	1-1	25601-1	EK80	Isfjorden	08:45			12:45	78°19.503	015°30.694	222	calibration of the 38 kHz frequency
04/09/2023	2-1	25602-1	SVP	Isfjorden	13:10	13:21	13:21	13:30	78°19.715	015°29.175	228	200 m sound velocity profile
04/09/2023	3-1	25603-1	Multibeam	all	15:30				78°21.883	015°42.046	194	hydroacoustic mapping during the entire cruise
05/09/2023	4-1	25604-1	CTD	Isfjorden	06:16	06:32	06:32	06:45	78°19.950	015°11.008	272	
05/09/2023	5-1	25605-1	MUC	Isfjorden	10:29	10:36	10:36	10:47	78°19.928	015°11.015	272	3/4 cores filled + 1/4 cores with lost sediments due to no proper closure, ~38 cm recovery
05/09/2023	6-1	25606-1	GC	Isfjorden	11:53	12:03	12:03	12:19	78°19.938	015°10.985	272	recovery 66 cm, accumulation of irregular shaped minerals in core catcher, H2S smell
05/09/2023	7-1	25607-1	SVP	Isfjorden	13:08	13:18	13:18	13:29	78°19.936	015°10.954	272	
06/09/2023	8-1	25608-1	GC	Isfjorden	06:21	06:29	06:28	06:42	78°19.940	015°10.977	273	recovery 254 cm, 3 m barrel, H2S smell
06/09/2023	9-1	25609-1	CTD	Isfjorden	07:59	08:14	08:14	08:23	78°19.887	015°40.424	98	
06/09/2023	10-1	25610-1	miniROV	Isfjorden	14:55			15:15	78°19.907	015°40.451	103	test, not into water
06/09/2023	11-1	25611-1	SVP	Nordfjorden	17:10	17:15	17:15	17:20	78°27.587	014°52.612	159	SVP down to 140 m

07/09/2023	12-1	25612-1	miniROV	Nordfjorden	06:35	06:46	09:11	09:25	78°29.267	014°46.083	120	microbial mats seen, no gas bubble sampling
07/09/2023	13-1	25613-1	CTD	Nordfjorden	09:48	10:01	10:01	10:18	78°29.262	014°46.055	120	max depth 2 m above seafloor deepest water sample 10 m above seafloor
07/09/2023	14-1	25614-1	GC	Nordfjorden	12:42	12:47	12:47	12:54	78°29.272	014°46.071	120	recovery 258 cm, 3 m barrel
07/09/2023	15-1	25615-1	SVP	Isfjorden	17:25	17:32	17:32	17:38	78°30.184	015°00.772	155	SVP down to 140 m
08/09/2023	16-1	25616-1	SonarLander	Nordfjorden	06:30	07:00			78°29.256	014°46.259	123	release time: 06:48:46 UTC
08/09/2023	17-1	25617-1	GC	Isfjorden	11:16	11:26	11:26	11:39	78°19.956	015°10.960	272	recovery 541 cm, 6 m barrel
08/09/2023	18-1	25618-1	SVP	Isfjorden	15:22	15:30	15:30	15:40	78°16.489	015°04.991	262	SVP down to 240 m, 2nd attempt
09/09/2023	19-1	25619-1	CTD	Isfjorden	06:10	06:23	06:23	06:35	78°15.036	014°39.403	223	
09/09/2023	20-1	25620-1	GC	Isfjorden	08:05	08:15	08:15	08:26	78°15.029	014°39.291	223	recovery 455 cm, 6 m barrel, lowermost ~4 cm of segment lost due to gas expansion
09/09/2023	21-1	25621-1	GC	Isfjorden	12:57	13:22	13:22	13:36	78°19.9477	015°10.9979	272	recovery 38 cm, 6 m barrel, corer fell probably off, strong H2S smell
09/09/2023	22-1	25622-1	GC	Isfjorden	14:12	14:28	14:28	14:57	78°19.9466	015°10.9974	273	recovery a few centimeters distributed in the liner, 3 m barrel
09/09/2023	23-1	25623-1	SVP	Isfjorden	16:32	16:40	16:40	16:55	78°26.419	015°44.709	254	SVP down to 230 m
10/09/2023	24-1	25624-1	SonarLander	Nordfjorden	06:03			06:48	78°29.308	14°45.994	119	recovery of lander
10/09/2023	25-1	25625-1	miniROV	Isfjorden	11:40	11:42	14:00	14:25	78°15.0326	14°39.3359	220	carbonates and microbial mats seen, termination due to technical issues
10/09/2023	26-1	25626-1	MUC	Isfjorden	14:35	14:47	14:47	15:01	78°15.0285	014°39.3501	226	4/4 filled cores
10/09/2023	27-1	25627-1	SVP	Isfjorden	15:45	15:56	15:56	16:08	78°15.185	014°32.910	268	SVP down to 240 m
11/09/2023	28-1	25628-1	SonarLander	Isfjorden	06:00	06:40			78°15.0287	014°39.3449	223	no camera

11/09/2023	29-1	25629-1	CTD	Isfjorden	07:28	07:39	07:39	07:54	78°15.098	014°24.869	289	background methane concentration, no flare
11/09/2023	30-1	25630-1	CTD	Isfjorden	11:06	11:17	11:17	11:37	78°11.7276	014°34.4068	187	
11/09/2023	31-1	25631-1	GC	Isfjorden	13:00	13:22	13:22	13:33	78°11.7282	014°34.4294	185	recovery 272 cm, 3 m barrel
11/09/2023	32-1	25632-1	SVP	Isfjorden	14:43	14:53	14:53	15:01	78°12.918	014°08.375	258	SVP down to 235 m
12/09/2023	33-1	25633-1	CTD	Prins Karls Forlandet	08:17	08:31	08:31	08:43	78°29.5109	010°31.4406	114	
12/09/2023	34-1	25634-1	GC	Prins Karls Forlandet	11:55	12:11	12:11	12:19	78°29.5117	010°31.4278	113	recovery 40 cm, 3 m barrel, strong smell like oil
12/09/2023	35-1	25635-1	GC	Prins Karls Forlandet	13:11	13:17	13:17	13:24	78°29.5571	010°31.4078	112	recovery 270 cm, 3 m barrel, strong smell of H2S
13/09/2023	36-1	25636-1	SVP	Kongsfjorden	01:56	02:07	02:07	02:19	78°57.443	011°54.952	358	2nd attempt
13/09/2023	37-1	25637-1	CTD	Prins Karls Forlandet	18:36	18:44	18:44	18:57	78°29.5666	010°31.4432	112	
14/09/2023	38-1	25638-1	CTD	Isfjorden	05:58	06:06	06:06	18:34	78°11.6351	014°05.9294	171	
14/09/2023	39-1	25639-1	MUC	Isfjorden	08:05	08:18	08:18	08:28	78°11.631	014°05.866	171	1/4 cores filled, no connection to GAPS system, lots of cm-sized debris
14/09/2023	40-1	25640-1	GC	Isfjorden	11:03	11:29	11:29	11:42	78°11.6334	014°05.844	174	recovery 217 cm, 3 m barrel, strong smell of H2S, gas expansion during sampling
14/09/2023	41-1	25641-1	GC	Isfjorden	13:01	13:21	13:21	13:31	78°11.6309	014°05.8864	173	recovery a few centimeters, 6 m barrel, core barrel bent
14/09/2023	42-1	25642-1	MUC	Isfjorden	13:58	14:36	14:36	14:44	78°11.6411	014°05.9086	173	3/4 cores filled and 1/4 cores filled without water column
15/09/2023	43-1	25643-1	SonarLander	Isfjorden	05:52			06:19	78°15.090	014°39.437	238	recovery of lander, no data recorded except CTD

15/09/2023	44-1	25644-1	MUC	Nordfjorden	08:43	08:51	08:51	08:57	78°29.2723	014°46.0525	120	3/4 cores filled and 1/4 cores filled without water column
15/09/2023	45-1	25645-1	miniROV	Isfjorden	11:21	11:48	11:48	13:54	78°15.472	015°18.954	209	pressure test
15/09/2023	46-1	25646-1	MUC	Isfjorden	15:03	15:07	15:07	15:21	78°19.9452	015°10.9856	273	3/4 cores filled, strong smell of H2S, mousse au chocolat texture
15/09/2023	47-1	25647-1	SVP	Isfjorden	17:08	17:16	17:16	17:22	78°26.035	015°40.519	258	SVP down to 230 m
16/09/2023	48-1	25648-1	SonarLander	Isfjorden	07:29	07:45			78°11.634	014°05.924	171	deployment of lander
16/09/2023	49-1	25649-1	SVP	Van Mijenfjorden	15:26	15:30	15:30	15:35	77°45.486	014°47.980	105	SVP down to 90 m
17/09/2023	50-1	25650-1	CTD	Van Mijenfjorden	06:26	06:36	06:36	06:54	77°45.5684	014°53.8066	111	
17/09/2023	51-1	25651-1	GC	Van Mijenfjorden	08:52	08:55	08:55	09:05	77°45.5565	014°53.7920	111	recovery 371 cm, 6 m barrel
17/09/2023	52-1	25652-1	MUC	Van Mijenfjorden	11:23	11:38	11:38	11:44	77°45.5573	014°53.7742	113	4/4 cores filled
17/09/2023	53-1	25653-1	SVP	Van Mijenfjorden	15:11	15:18	15:18	15:22	77°47.883	015°45.378	85	SVP down to 65 m
18/09/2023	54-1	25654-1	CTD	Van Mijenfjorden	06:10	06:21	06:21	06:42	77°44.5964	015°04.6906	106	
18/09/2023	55-1	25655-1	MUC	Van Mijenfjorden	08:23	08:30	08:30	08:35	77°44.5988	015°04.6934	106	3/4 cores filled
18/09/2023	56-1	25656-1	GC	Van Mijenfjorden	11:02	11:12	11:12	11:22	77°44.5980	015°04.6890	108	recovery 431 cm
18/09/2023	57-1	25657-1	CTD	Van Mijenfjorden	13:09	13:31	13:31	14:07	77°47.3694	015°41.1655	83	water sample at 65 m about 20 m distance to flare
18/09/2023	58-1	25658-1	MUC	Van Mijenfjorden	15:14	15:33	15:33	15:37	77°47.3678	015°41.1771	81	3/4 cores filled
19/09/2023	59-1	25659-1	GC	Van Mijenfjorden	06:03	06:12	06:12	06:21	77°47.3692	015°41.1769	80	recovery 359 cm, ~ 10 cm sediment loss at 72 cm core depth during retrieval
20/09/2023	60-1	25660-1	SVP	Isfjorden	04:08	04:17	04:17	04:23	78°13.286	014°10.557	276	
20/09/2023	61-1	25661-1	SonarLander	Isfjorden	06:05			06:32	78°11.668	014°05.885	171	recovery of lander
20/09/2023	62-1	25662-1	CTD	Isfjorden	13:44	15:57	15:57	14:17	78°15.039	014°39.379	222	without Posidonia due to technical problems with power supply
20/09/2023	63-1	25663-1	SonarLander	Isfjorden	14:30	14:43			78°15.0305	014°39.3468	221	deployment of lander

20/09/2023	64-1	25664-1	CTD	Isfjorden	15:47	16:00	16:00	16:19	78°16.0584	014°59.5824	223	bottle #10 not closed as lids were blocked by the winch cable
21/09/2023	65-1	25665-1	CTD	Billefjorden	06:07	06:17	06:17	06:33	78°35.692	016°30.415	163	no flare position, bottle #11 not closed as lids were blocked by winch cable
21/09/2023	66-1	25666-1	MUC	Billefjorden	08:36	08:42	08:42	08:49	78°35.688	016°30.459	161	3/4 cores filled, without GAPS
21/09/2023	67-1	25667-1	CTD	Isfjorden	12:04	12:25	12:25	12:58	78°19.9477	015°10.9630	268	
21/09/2023	68-1	25668-1	GC	Isfjorden	13:46	13:59	13:59	14:14	78°19.9459	015°10.9817	269	recovery 539 cm
22/09/2023	69-1	25669-1	CTD	Nordfjorden	06:20	06:31	06:31	06:46	78°23.9463	015°06.1289	174	
22/09/2023	70-1	25670-1	CTD	Isfjorden	07:51			08:49	78°19.9509	015°10.9167	272	cross over flare cluster, all water samples from about 262 m water depth
22/09/2023	71-1	25671-1	GC	Isfjorden	11:02	11:21	11:21	11:36	78°19.9425	015°10.9841	269	recovery 367 cm
23/09/2023	72-1	25672-1	CTD	Isfjorden	09:43	09:59	09:59	10:17	78°09.9150	013°47.6348	424	water samples in depths between 208 m and 415 m
23/09/2023	73-1	25673-1	CTD	Isfjorden	10:28	10:41	10:41	10:58	78°09.9271	013°47.7221	423	water samples in depths between 8 m and 260 m
23/09/2023	74-1	25674-1	SonarLander	Isfjorden	12:37			13:31	78°15.040	014°39.046	229	recovery of lander
23/09/2023	75-1	25675-1	CTD	Isfjorden	15:02	15:17	15:17	15:34	78°21.1673	015°21.7378	259	
23/09/2023	76-1	25676-1	SVP	Sassenfjorden	18:35			18:40	78°22.170	016°49.011	96	failure
24/09/2023	77-1	25677-1	SVP	Sassenfjorden	00:49	00:52	00:52	00:55	78°22.313	016°33.924	86	
24/09/2023	78-1	25678-1	SVP	Adventfjorden	05:03	05:11	05:11	05:17	78°17.345	015°26.074	254	SVP down to 230 m
24/09/2023	79-1	25679-1	MUC	Adventfjorden	06:20	06:25	06:25	06:29	78°14.9525	015°35.6907	72	failure
24/09/2023	80-1	25680-1	MUC	Adventfjorden	06:34	06:36	06:36	06:40	78°14.9526	015°35.6821	72	3/4 cores filled, repetition of MUC-11

6.2 Survey List

Survey Number	Area	Start	End	Vessel speed (kn)	Objective/Result
Mapping Box 1	Isfjorden	20230904_152713	20230904_224300	5	Over 38 flares/flare clusters
Transit	Isfjorden	20230904_224300	20230904_234700		Between MB 1-2
Mapping Box 2	Isfjorden	20230904_234700	20230905_060600	5	Noisy data. Strong flares. Very shallow mode used.
Mapping Box 2 V2	Isfjorden	20230905_140307	20230905_211919	5	Repeat data acquisition with MBEs in Shallow mode. 31 flares
Transit	Isfjorden	20230905_211920	20230905_220949		Between MB 2-3. Flares observed
Mapping Box 3	Isfjorden	20230905_220949	20230906_052607	5	Over 49 flares/flare clusters. MBEs in Shallow mode
Mapping Box 4	Isfjorden	20230906_174327	20230907_010244	5	Over 78 flares/flare clusters. MBEs in Shallow mode
Mapping Box 5	Isfjorden	20230907_011750	20230907_054921	5	Over 57 flares/flare clusters. MBEs in Shallow mode
Mapping Box 5 V2	Isfjorden	20230907_180024	20230907_205345	5	Over 7 flares/flare clusters. MBEs in Shallow mode
Mapping Box 6	Isfjorden	20230907_210622	20230908_042000	5	One flare
Transit	Isfjorden	20230908_053041	20230908_060327		Between MB 5 and station 16
Mapping Box 7	Isfjorden	20230908_160133	20230908_231823	5	Over 19 flares/flare clusters. MBEs in Shallow mode
Transit	Isfjorden	20230908_231914	20230909_000538	7	Between MB 7-8. Several flares
Mapping Box 8	Isfjorden	20230909_000720	20230909_054126	5	Over 21 flares/flare clusters. MBEs in Shallow mode
Transit	Isfjorden	20230909_090841	20230909_111004	7	Between MB 8-2. 3 Flares
Transit	Isfjorden	20230909_145937	20230909_163200	6.6	Between MB 2-10. 7 Flares
Mapping Box 9	Isfjorden	20230909_172508	20230910_003154	5	No flares. MBEs in Very Shallow mode
Mapping Box 10	Isfjorden	20230910_004848	20230910_041846	5	1 potential flare. MBEs in Shallow mode
Transit	Isfjorden	20230910_041933	20230910_060309	7	Between MB 10 and Station 10. 5 Flares
Transit	Isfjorden	20230910_065015	20230910_085212		Between Station 10 and MB 8. 5 Flares
Mapping Box 8 V2	Isfjorden	20230910_164000	20230910_181452	5	9 flares/flare clusters described
Transit	Isfjorden	20230910_182415	20230910_183713		Between MB 8-11. 2 flares observed
Mapping Box 11	Isfjorden	20230910_183713	20230911_015609	5	9 flares/flare clusters described

Transit	Isfjorden	20230911_015724	20230911_023710	7	Between MB 11-12. 1 flare observed
Mapping Box 12	Isfjorden	20230911_023713	20230911_050737	5	No flares
Transit	Isfjorden	20230911_050804	20230911_054357		Between MB 12 and Station 28. 3 flares observed
Transit	Isfjorden	20230911_065359	20230911_072536		Between Station 28-29. No flares observed
Transit	Isfjorden	20230911_134114	20230911_143422	7	Between MB 11-13. 1 flare observed
Mapping Box 13	Isfjorden	20230911_151744	20230911_223543	5	Over 45 flares/flare clusters
Transit	Prins Karls Forland	20230911_223655	20230912_060942	7	To Prins Karls Forland
Mapping Box PKF	Prins Karls Forland	20230912_060942	20230912_112720	5	Over 24 flares/flare clusters. CTD Station 33 made during the mapping
Transit	Prins Karls Forland	20230912_161055	20230912_182033	6	Between MB PKF-Kongsfjorden. 89 flares observed
Mapping Box Kongsfjorden	Kongsfjorden	20230913_023956	20230913_054949	5	No flares observed
Mapping Box Kongsfjorden V2	Kongsfjorden	20230913_091108	20230913_132330	5	No flares observed
Transit	Prins Karls Forland	20230913_132331	20230913_183306	7	Between MB Kongsfjorden-PKF
Transit	Isfjorden	20230913_202440	20230914_042454	7	Between Station 37 (PKF)-Station 38 (Isfjorden)
Exploratory	Trygghamna	20230914_0838	20230914_105321	5	Exploratory fjord in Trygghamna. MBEs in Shallow mode
Exploratory	Ymmerbukta	20230914_145808	20230914_173418		Exploratory fjord in Ymmerbukta. MBEs in Very Shallow mode
Mapping Box 14	Isfjorden	20230914_181429	20230915_012823	5	Over 9 flares/flare clusters. Runtime parameters changed to max angle ±48 deg and swath ±210 m
Mapping Box 15	Isfjorden	20230915_013247	20230915_041549	5	2 flares observed. Runtime parameters changed to max angle ±65 deg and swath ±500 m
Transit	Isfjorden	20230915_041549	20230915_042111		Between MB 15-8. 6 Flares
Transit	Isfjorden	20230915_055223	20230915_062259	7	Between MB 8-4. Flares observed
Mapping Box 10 V2	Isfjorden	20230915_174410	20230915_211518	5	7 flares observed
Mapping Box 16	Isfjorden	20230915_212436	20230916_043158	5	Over 45 flares/flare clusters
Transit	Isfjorden	20230916_044643	20230916_072510		Between MB 16-8. 4 Flares
Transit	Van Mijenfjorden	20230916_074840	20230916_151925	7	MBEs in Shallow mode

Mapping Box 17	Van Mijenfjorden	20230916_154036	20230916_232034	5	Over 22 flares/flare clusters
Mapping Box 18	Van Mijenfjorden	20230916_233648	20230917_062052	5	6 questionable flares observed
Mapping Box 19	Van Mijenfjorden	20230917_130939	20230917_212135	5	Over 29 flares/flare clusters. Station 53, SVP 11 made during the mapping
Mapping Box 20	Van Mijenfjorden	20230917_214045	20230918_051347	5	3 doubtful flares
Exploratory	Rindersbukta	20230918_155005	20230918_184913		No flares
Mapping Box 21	Van Mijenfjorden	20230918_2134	20230919_011751	5	Over 9 flares/flare clusters
Mapping Box 18 V2	Van Mijenfjorden	20230919_020730	20230919_032220	5	No flares
Transit	Van Keulenfjorden	20230919_064705	20230919_103659	8	No flares. Did not go into Fritjovhamna
Exploratory	Van Keulenfjorden	20230919_103659	20230919_144854	5	Over 13 flares/flare clusters
Transit	Isfjorden	20230919_171454	20230920_005535		Strong flares at the entrance of Isfjorden
Mapping Box 22	Isfjorden	20230920_005812	20230920_054608	5	Over 8 flares/flare clusters. Station 60, SVP 13 made during the mapping
Exploratory	Grønfjorden	20230920_072850	20230920_095004	5	4 flares observed
Transit	Billefjorden	20230920_172207	20230920_212433	6	13 flares observed along Isfjorden
Mapping Box 23	Billefjorden	20230920_212433	20230921_043342	5	No clear flares. Noisy water column data
Exploratory	Adolfbukta	20230921_063335	20230921_075552	5	5 potential flares
Transit	Isfjorden	20230921_085346	20230921_114916		Between MB 23-2. 5 Flares
Mapping Box 2 V3	Isfjorden	20230921_144817	20230921_193714	5	Repetition of MB 2. Over 35 flares/flare clusters
Transit	Isfjorden	20230921_193840	20230921_201320	5	Between MB 2-24
Mapping Box 24	Isfjorden	20230921_201320	20230922_031955	5	Over 91 flares/flare clusters
Exploratory	Forlandssundet	20230922_114155	20230923_075927	8	Over 12 flares/flare clusters
Mapping Box 25	Sassenfjorden	20230923_185303	20230924_003647	5	No flares observed
Transit	Isfjorden	20230924_012524	20230924_0502	5	Over 12 flares/flare clusters
Mapping Box 26	Adventfjorden	20230924_052801		5	No flares observed

7 Data and Sample Storage and Availability

All digital data collected during the cruise will be stored and archived at the PANGAEA information system sustained by the World Data Center for Marine Environmental Sciences (WDC-MARE) in Bremen. All gas, sediment and pore water samples are stored under appropriate conditions at the MARUM in Bremen. Gas and pore water samples will be kept in glass vials or flasks in the cooling room (4°C). Sediment cores are stored in the MARUM core repository at 4°C.

Table 7.1: List of data acquired during HE628 with database and contact information.

Data Type	Database	Available	Open Access	Contact
Innomar SES2000	PANGAEA	04/2024	10/2026	Evgenia Bazhenova (ebazhenova@marum.de)
Kongsberg EM710	PANGAEA	04/2024	10/2026	Evgenia Bazhenova (ebazhenova@marum.de)
Simrad EK80	PANGAEA	04/2024	10/2026	Evgenia Bazhenova (ebazhenova@marum.de)
MiniROV video data	MARUM	10/2023	10/2026	Ralf Bachmayer (rbachmayer@marum.de)
ICOS data	PANGAEA	04/2024	10/2026	Miriam Römer (mroeme@marum.de)
CTD data	PANGAEA	04/2024	10/2026	Thomas Pape (tpape@marum.de)
Sediment cores	MARUM	10/2023	10/2023	Thomas Pape (tpape@marum.de)
Sonar.81A binary files, PlasPI footage, CTD data	PANGAEA	04/2024	10/2026	Yann Marcon (ymarcon@marum.de)

8 Acknowledgements

Overall, the cruise has been very successful and we look forward to analysing the samples and data acquired. It was a pleasure to work on R/V HEINCKE and we would like to thank the captain and his team who contributed considerably to making this cruise a success. They supported us fully during all stations, always making sure that everything was as we wished for. Extraordinary thanks are due to the boatswain as well as the team on the work deck and below for their ongoing, valuable, courteous and friendly support. We also want to thank the logistics and research platforms department at the AWI for organizing and supporting the realization of our cruise. And it was of great help that we were allowed to use polar clothes from the clothing store. For financial support, we thank MARUM - Center for Marine Environmental Sciences, University of Bremen through an „Incentive Funds“ of the Cluster of Excellence „Ocean Floor".

9 References

Abay, T.B., Karlsen, D.A., Lerch, B., Olaussen, S., Pedersen, J.H. & Backer-Owe, K. 2017. Novel proof of Migrated Petroleum in the Mesozoic strata in Svalbard and detailed Organic Geochemical Characterization-Implications for Regional Exploration. Journal of Petroleum Geology 40, 5–36. https://doi.org/10.1111/jpg.12662

Belsare et. al. (2023). Micro-ROS. In A. Koubaa, Robot Operating System (ROS) (S. 3-55). Springer Cham.

Betlem, P., Roy, S., Birchall, T., Hodson, A., Noormets, R., Römer, M., Skogseth, R., Senger, K., 2021. Modelling of the gas hydrate potential in Svalbard's fjords, Journal of Natural Gas Science and Engineering, 94,104127, https://doi.org/10.1016/j.jngse.2021.104127.

Bohrmann G., Torres M.E., 2006. Gas Hydrates in Marine Sediments. In: Schulz H.D., Zabel M. (eds) Marine Geochemistry. Springer, Berlin, Heidelberg. https://doi.org/10.1007/3-540-32144-6_14.

Borowski, W.S., Paull, C.K. and Ussler III, W., 1996. Marine pore-water sulfate profiles indicate in situ methane flux from underlying gas hydrate. Geology 24, 655-658.

Gentz, T., Damm, E., Schneider von Deimling, J., Mau, S., McGinnis, D.F. and Schlüter, M., 2014. A water column study of methane around gas flares located at the West Spitsbergen continental margin. Cont. Shelf Res. 72, 107-118.

Gutiérrez-Flores, P. A., & Bachmayer, R., 2022. Concept development of a modular system for marine applications using ROS2 and micro-ROS. IEEE/OES Autonomous Underwater Vehicles Symposium (AUV), (S. 1-6). Singapur.

Macenski, S., Foote, T., Gerkey, B., Lalancette, C., & William, W., 2022. Robot Operating System 2: Design, architecture, and uses in the wild. Science Robotics vol. 7.

Marcon Y., Kopiske, E., Leymann, T., Spiesecke, U., Vittori, V., von Wahl, T., et al., 2019. A Rotary Sonar for Long-Term Acoustic Monitoring of Deep-Sea Gas Emissions. OCEANS 2019 - Marseille, 2019, pp. 1-8, doi: 10.1109/OCEANSE.2019.8867218.

Marcon, Y., Kelley, D., Thornton, B., Manalang, D., & Bohrmann, G., 2021. Variability of natural methane bubble release at Southern Hydrate Ridge. Geochemistry, Geophysics, Geosystems, 22, e2021GC009894. https://doi.org/10.1029/2021GC009894

Mau, S., Römer, M., Torres, M.E., Bussmann, I., Pape, T., Damm, E., Geprägs, et al., 2017. Widespread methane seepage along the continental margin off Svalbard - from Bjørnøya to Kongsfjorden. Scientific Reports, 7. 42997. doi:10.1038/srep42997.

Mau, S., Tu, T.-H., Becker, M., dos Santos Ferreira, C., Chen, J.-N., Lin, L.-H., Wang, P.-L., Lin, S. and Bohrmann, G., 2020. Methane seeps and independent methane plumes in the South China Sea offshore Taiwan. Frontiers in Marine Science 7.

Ohm, S.E., Larsen, L., Olaussen, S., Senger, K., Birchall, T., Demchuk, T., et al., 2019. Discovery of shale gas in organic rich Jurassic successions, Adventdalen, Central Spitsbergen, Norway. Norwegian Journal of Geology 99. doi:dx.doi.org/10.17850/njg007.

Pape, T., Bünz, S., Hong, W.-L., Torres, M.E., Riedel, M., Panieri, G., Lepland, A., Hsu, C.W., Wintersteller, P., Wallmann, K., Schmidt, C., Yao, H. and Bohrmann, G., 2020. Origin and transformation of light hydrocarbons ascending at an active pockmark on Vestnesa Ridge, Arctic Ocean. J. Geophys. Res.-Sol. Ea. 125.

Purser, A., Hoge, U., Lemburg, J., Bodur, Y., Schiller, E., Ludszuweit, J., Greinert, J., Dreutter, S., Dorschel, B., Wenzhöfer, F., 2020. PlasPI marine cameras: Open-source, affordable camera systems for time series marine studies. HardwareX 7, e00102. https://doi.org/10.1016/j.ohx.2020.e00102.

Rodes, N., Betlem, P., Senger, K., Römer, M., Hodson, A., Liira, M., Birchall, T., Roy, S., Noormets, R., Smyrak-Sikora, A., Olaussen, S. and Bohrmann, G., 2023. Active gas seepage in western Spitsbergen fjords, Svalbard archipelago: spatial extent and geological controls. Front. Earth Sci. 11:1173477. doi: 10.3389/feart.2023.1173477

Römer, M., Sahling, H., Pape, T., Spiess, V., Bohrmann, G., 2012. Gas bubble emission from submarine hydrocarbon seeps at the Makran continental margin (offshore Pakistan). Journal of Geophysical Research, 117, C10015, doi:10.1029/2011JC007424.

Römer, M., Riedel, M., Scherwath, M., Heesemann, M. and Spence, G.D., 2016. Tidally controlled gas bubble emissions: A comprehensive study using long-term monitoring data from the NEPTUNE cabled observatory offshore Vancouver Island. Geochemistry, Geophysics, Geosystems, 17(9). 3797-3814. doi:10.1002/2016GC006528.

Römer, M. et al., 2021. Variability, amount and fate of methane seepage in the German North Sea, Cruise No. MSM98, 08.01.2021 - 23.01.2021, Emden (Germany) - Emden (Germany). GPF, https://doi.org/10.48433/cr_msm98.

Roy, S., Hovland, M., Noormets, R., Olaussen, S., 2015. Seepage in Isfjorden and its tributary fjords, West Spitsbergen. Marine Geology 363, 146-159.

Roy, S., Senger, K., Hovland, M., Römer, M., Braathen, A., 2019. Geological controls on shallow gas distribution and seafloor seepage in Arctic fjord of Spitsbergen, Norway. Marine and Petroleum Geology. 107, 237-254. https://doi.org/10.1016/j.marpetgeo.2019.05.021.

Sahling, H., Römer, M., Pape, T., Bergès, B., dos Santos Ferreira, C., Boelmann, J., et al., 2014. Gas emissions at the continental margin west of Svalbard: mapping, sampling, and quantification. Biogeosciences, 11(21): 6029-6046.

Schneider von Deimling, J., Brockhoff, J., and Greinert, J., 2007. Flare imaging with multibeam systems: Data processing for bubble detection at seeps, Geochem. Geophys. Geosyst., 8, Q06004, doi:10.1029/2007GC001577.

Senger, K., Brugmans, P., Grundvåg, S.-A., Jochmann, M., Nøttvedt, A., Olaussen, S., et al., 2019. Petroleum, coal and research drilling onshore Svalbard: A historical perspective. Norwegian Journal of Geology 99. doi:10.17850/njg99-3-1

Spencer, A.M., Briskeby, P.I., Christensen, L.D., Foyn, R., Kjolleberg, M., Kvadsheim, E., Knight, I., Rye-Larsen, M., and Williams, J., 2008, Petroleum geoscience in Norden—Exploration, production and organization: Episodes, v. 31, p. 115–124, https://doi.org/10.18814/epiiugs/2008/v31i1/016.

Veloso, M., Greinert, J., Mienert, J., De Batist, M., 2015. A new methodology for quantifying bubble flow rates in deep water using splitbeam echosounders: Examples from the Arctic offshore NW-Svalbard. Limnol. Oceanogr. Methods, 13: 267-287. https://doi.org/10.1002/lom3.10024.